ETS IN TIDAL RECORDS

by

SEQUOIA ALBA

A THESIS

Presented to the Department of Geological Sciences
and the Graduate School of the University of Oregon
in partial fulfillment of the requirements
for the degree of
Master of Science

December 2011

THESIS APPROVAL PAGE

Student: Sequoia Alba

Title: ETS in Tidal Records

This thesis has been accepted and approved in partial fulfillment of the requirements for the Master of Science degree in the Department of Geological Sciences by:

Dr. David A. Schmidt	Chair
Dr. Ray J. Weldon	Advisor
Dr. Dean Livelybrooks	Member

and

Kimberly Andrews Espy	Vice President for Research and Graduate Studies/ Dean of the Graduate School

Original approval signatures are on file with the University of Oregon Graduate School.

Degree awarded December 2011

THESIS ABSTRACT

Sequoia Alba

Master of Science

Department of Geological Sciences

December 2011

Title: ETS in Tidal Records

Uplift rates associated with 12 episodic tremor and slip events on the Cascadia Subduction Zone occurring between 1997 and 2010 have been determined from hourly water level records from 4 NOAA tide gauges (Neah Bay, Port Angeles, Port Townsend, and Seattle). Displacements inferred from water levels generally agree with displacements inferred from modeling GPS data. Examination of uplift between events shows an inter-event deformation rate approximately equal in magnitude, with ETS events, on average, releasing strain accumulated between events, suggesting that ETS is consistent with the elastic rebound theory. Additionally, while the GPS record only extends to the late 1990s and the tremor record includes only recent decades for Cascadia, tidal records in the Pacific Northwest and around the world span many decades. Thus, by showing that ETS can be resolved in tidal records we open up the possibility that tidal records could be used to study ETS where other tools are not available.

This thesis includes unpublished coauthored material.

CURRICULUM VITAE

NAME OF AUTHOR: Sequoia Alba

GRADUATE AND UNDERGRADUATE SCHOOLS ATTENDED:
University of Oregon, Eugene, Oregon
Portland State University, Portland, Oregon

DEGREES AWARDED:
Master of Science in Geology, 2011, University of Oregon
Bachelor of Science in Physics, 2008, University of Oregon
Bachelor of Arts in Spanish Language and Literature, 2003, Portland State
University

AREAS OF SPECIAL INTEREST:
Geophysics, Neotectonics, Geophysical Instrumentation

PROFESSIONAL EXPERIENCE:

Graduate Research Assistant, Department of Geological Sciences, University of
Oregon, Eugene, Oregon, 2010-2011

Graduate Teaching Fellow, Department of Geological Sciences, University of
Oregon, Eugene, Oregon, 2009

Research Assistant, Department of Geological Sciences, University of Oregon,
Eugene, Oregon, 2005-2009

Lab Assistant, General Physics Teaching Laboratory, University of Oregon,
Eugene, Oregon, 2005-2009

GRANTS, AWARDS AND HONORS:

Graduate Teaching Fellowship, University of Oregon Department of Geological
Sciences, 2009-2011

Outstanding Student Employee, University of Oregon Department of Physics,
2008

PUBLICATIONS:

Gaskell, P. E., J. J. Thorn, S. Alba, and D. A. Steck (2009). An open-source, extensible system for laboratory timing and control, *Rev. Sci. Inst.*, *80*, 115–125.

ACKNOWLEDGEMENTS

I would like to thank a number of people for their contribution to this thesis and to my development as a scientist. First and foremost my advisor, Dr. Ray Weldon, who encouraged me to make the switch from physics to geology. I thank him for all the many hours of talking through problems with me, for answering all my rudimentary questions about geology with tact and enthusiasm, for his brilliance, his dedication to science, and for making me feel like my advisor is a rock star whenever he gives a speech.

I would like to thank the other members of my committee, David Schmidt and Dean Livelybrooks, for all their helpful suggestions. I would especially like to thank Dr. Livelybrooks for helping me get my first job with Dr. Weldon when I was an undergraduate in physics. Dr. Schimdt's students were also endlessly helpful, providing GPS modeling data, and interesting conversation.

I am deeply grateful to Aaron Webster, my husband, who continues to encourage me to value my skepticism and scientific integrity above all. You have spent so many hours volunteering to help me solve a tricky problem, talk through something, or teach me how to code. Your enthusiasm is infectious and inspiring. Your jokes always make me laugh. You are pretty much my hero and I love you.

I can live with doubt, and uncertainty, and not knowing. I think it's much more interesting to live not knowing than to have answers which might be wrong. I have approximate answers, and possible beliefs, and different degrees of certainty about different things, but Im not absolutely sure of anything, and in many things I dont know anything about, such as whether it means anything to ask why were here, and what the question might mean.

Richard Feynman

TABLE OF CONTENTS

LIST OF FIGURES

LIST OF TABLES

CHAPTER I

INTRODUCTION

The greatest source of seismic hazard in the US is the Cascadia Subduction Interface. In addition to megathrust earthquakes, it has recently been discovered that very slow earthquakes also occur on the fault. Accompanied by subseismic tremor, they occur over days to weeks and recur with near periodicity. Dense GPS and seismic arrays have thus far been the main tools utilized in the study of this phenomenon. This thesis presents the use of tide gauge records for the study of episodic tremor and slip, or ETS, in Cascadia.

1.1. Cascadia Convergence and Slow Earthquakes

From west to east, the Cascadia Subduction Zone consists of a sediment filled trench formed as the Juan de Fuca, Explorer, and Gorda oceanic plates (henceforth referred to simply as the Juan de Fuca plate, or JDF) bends and slides beneath the overlying North American continental plate [*Wells and Simpson*, 2001]. Landward of the trench is a locked zone, a section of the plate boundary where North America and the Juan de Fuca plates are locked. In the locked zone, plate convergence is accommodated in a stick-slip cycle of long periods of slip deficit (as North America sticks to the down going plate), followed by large earthquakes during which all the relative plate motion occurs in seconds to minutes in a catastrophic megathrust earthquake.

The convergence rate between North America and the Juan de Fuca plate is $\sim 4\,\text{cm/yr}$ and geodetic and geologic studies have concluded that the Cascadia Subduction Zone is locked and accumulating strain [*Savage et al.*, 1991; *Burgette*

1

et al., 2009]. Downdip of the fully locked zone, or eastward on a surficial projection, the plates are siding freely past each other. Between the locked and freely slipping zones is a transition zone[1]. It has previously been defined simply as a mathematical taper to address the necessity for there to be some transition between the brittle seismogenic zone and the ductile zone of steady creep rather than by any particular observed behavior unique to the transition zone itself. The exact depth of the updip and downdip extent of the transition zone, and by extension the inland extent of the seismogenic zone have been the subject of some debate but have been proposed to be $\sim 10\,\text{km}$ to $15\,\text{km}$ and $\sim 20\,\text{km}$ to $35\,\text{km}$ respectively in northern Cascadia [*Wang et al.*, 2003; *McCaffrey et al.*, 2007; *Burgette et al.*, 2009]. The study of ETS, which takes place along the fault in the transition zone or immediately below, can help better define the inland extent of the megathrust seismogenic zone.

Since the discovery of transient slip inferred from GPS time series [*Dragert et al.*, 2001] and associated tremor [*Rogers and Dragert*, 2003], much work has been done to understand and classify ETS in Cascadia. Inversions of GPS horizontal displacements result in estimates for slip magnitude and inter-event timing for slip located on the plate interface. Slip migrates along strike, and is modeled as moving from the epicenter of an event over the course of several weeks at a rate of $\sim 6\,\text{km}$ to $17\,\text{km}$ per day [*Schmidt and Gao*, 2010]. Events occur approximately every 14 months and last from ~ 7 to 30 days [*Szeliga et al.*, 2008; *Wech et al.*, 2009].

Tide gauges at the shoreline can be used to estimate vertical tectonic displacements of the land. Vertical displacement patterns are very useful in locating the downdip extent of slip. However, coastal water levels are highly variable, subject to the effects astronomical tides, meteorological effects, seasonal variations, and even

---

[1]Other models, especially *McCaffrey et al.* [2007] solve for a degree of locking parameter rather than locked, tapered, and freely slipping zones.

long period oscillations from ocean basins and global cycles. Long term tectonic uplift in Cascadia and other places has been successfully estimated using tide gauge data, but long records are required to overcome the daunting signal to noise ratio. *Burgette et al.* [2009] presented a method of comparing records from neighboring sites in a pairwise fashion which results in a rough removal of shared noise. This allowed for estimates of uplift from short records with errors similar to those previously produced only with very long (many decades) records. We have adapted the methods of *Burgette et al.* [2009], with additional signal processing to further reduce shared noise so that we can estimate uplift during ETS events using short records.

1.2. Format and Organization

Chapter II of this thesis is an unpublished co-authored article in the format of the peer reviewed journal, Nature Geoscience, which is a complete, though abbreviated report of the research done on ETS from tide gauge records. Due to the necessarily abbreviated nature of a journal article, I include additional chapters which expand on the information covered briefly in the Methods section of the journal article, and provides a more detailed treatment of the data analysis methods used, as well as some assessment of the efficacy of these methods.

Chapter II focuses mostly on the results of our study, the actual estimates of average vertical deformation associated with the ETS seismic cycle, and how those results compare with the GPS estimates and fit with current tectonic models. This thesis, with the addition of the supplemental chapters on methodology, also describes and compares the two methods I applied to remove shared noise. Chapter III, Data Analysis, describes the methods used to remove noise and estimate uplifts from tide

gauge records. Chapter IV, Error, explores the estimation of uncertainty on estimated

uplifts and compares different processing methods.

CHAPTER II

ETS EARTHQUAKES ON THE CASCADIA SUBDUCTION ZONE

SEEN IN TIDAL RECORDS

The procedure described in this chapter was developed by a number of workers, including my advisor, Dr. Ray J. Weldon. Dr. Weldon contributed substantially to this work by participating in the development of a standard procedure for data processing. Dr. Livelybrooks developed the transfer function approach to noise removal and wrote Matlab code for its implementation. Dr. Schmidt provided GPS modeling for comparison. I was the primary contributor to the development, implementation, and analysis of a procedure for producing inferred uplifts from tide gauge records. I developed the wavelet approach to noise removal, wrote all the code except that written by Dr. Livelybrooks, and did all the writing.

2.1. Introduction

Vertical displacements, uplift rates between events, and net uplift rates spanning the most recent 12 episodic tremor and slip events (ETS) on the northern Cascadia Subduction Zone (that occurred beneath the Olympic Peninsula, WA, between 1997 and 2010) have been determined from hourly water level records from 4 NOAA tide gauges (Neah Bay, Port Angeles, Port Townsend, and Seattle). This time period, which is essentially that covered by GPS, was chosen to assess the ability of such data to accurately record ETS events. Displacements inferred from water level measurements, during individual events, are on the order of millimeters with near centimeter uncertainties, whereas 12 event average displacements by site are resolved to 1-2 mm (-1.35 ± 1.50 mm at Neah Bay, 3.86 ± 1.29 mm, Port Angeles,

-2.38 ± 1.22 mm, Port Townsend, and -0.13 ± 1.78 mm at Seattle), which generally agree with displacements inferred from modeling GPS data. Additionally, while the GPS record only extends to the late 1990s and the seismic record of tremor includes only recent decades for Cascadia, there are tidal records in the Pacific Northwest and around the world spanning many decades and in some cases more than a century. Thus, by showing that ETS can be resolved in tidal records we open up the possibility that tidal records could be used to study ETS in regions and time periods not covered my extensive GPS or seismic arrays.

2.2. Background

The Cascadia Subduction Zone, which forms the convergent boundary between the North American continental plate and the Gorda, Juan de Fuca, and Explorer oceanic plates, generates catastrophic megathrust earthquakes, the last of which was in 1700 AD [*Nelson et al.*, 1995; *Satake et al.*, 1996; *Jacoby et al.*, 1997; *Yamaguchi et al.*, 1997]. Megathrust earthquakes, like the Sumatra earthquake of 2004, and recent devastating 2011 Tōhoku earthquake in Japan, can cause extensive damage and loss of life in areas of high human population if appropriate engineering and planning are not in place. They pose the greatest natural hazard to the people of the Pacific Northwest. Although the megathrust cycle is the most visible and dangerous tectonic process associated with subduction, another, quieter phenomenon has been recently discovered, slow earthquakes. Slow earthquakes, which are accompanied by non-volcanic seismic tremor and slip (sometimes called episodic tremor and slip, or ETS), occur at near regular intervals, and have been identified by both GPS arrays and seismic data[*Dragert et al.*, 2001; *Miller et al.*, 2002; *Rogers and Dragert*, 2003]. The study of slow earthquakes may provide insight into physical processes occurring

below the locked zone on the interface between plates and, possibly, implications for future megathrust events.

ETS, since its discovery in the Nankai region of Japan [*Hirose et al.*, 1999; *Obara*, 2002] and in northern Cascadia [*Dragert et al.*, 2001; *Miller et al.*, 2002; *Rogers and Dragert*, 2003] has been found in other subduction zones [*Obara et al.*, 2004; *Schwartz and Rokosky*, 2007; *Payero et al.*, 2008; *Gomberg and et al.*, 2010] and the San Andreas Fault [*Shelly et al.*, 2006]. Aside from indicating a need to reevaluate our current understanding of tectonic processes in subduction zones. This could have a great effect on hazard assessment for those residing near subduction zones. Specifically, the location of ETS related slip along the fault may help define the landward extent of the seismogenic zone [*Chapman and Melbourne*, 2009] during megathrust events, an ETS event may trigger a megathrust event [*Gomberg and et al.*, 2010], or changes in ETS size or frequency may occur through the megathrust seismic cycle [*Matsuzawa et al.*, 2010].

Thus far, dense GPS networks have been the primary tool to measure surface displacement during ETS. Several workers have published inversions of observed surface displacements associated with recent ETS events to map slip distributions onto the subduction interface [*McGuire and Segall*, 2003; *Szeliga et al.*, 2004; *Melbourne et al.*, 2005; *Wang et al.*, 2003; *Szeliga et al.*, 2008; *McCaffrey et al.*, 2007; *Schmidt and Gao*, 2010]. Distributed slip inversions show a maximum uplift located beneath the NE edge of the Olympic Peninsula near the town of Port Angeles, Washington (Figure 2.1.). The average slip per event is on the order of a few centimeters. However, GPS has relatively poor vertical resolution, and vertical displacements are particularly useful in locating the downdip (and therefore inland) extent of slip as well as the distribution of the magnitude of slip on the slip patch. Tidal records from

the 4 main NOAA stations in NW Washington, spanning more than 15 years from 1996 to 2011, are used here to estimate vertical deformation during recent ETS in Northern Cascadia. This time period, which is essentially that covered by GPS and can therefore be compared to GPS measurements, was chosen to assess the ability of such data to accurately record ETS events. GPS and seismic records only extend back a couple of decades, whereas, there are tidal records in the Pacific Northwest and around the world spanning many decades and in some cases more than a century. If ETS related uplifts can be reliably measured using tide gauge data we can look back in time in Cascadia and discover how ETS changes through the megathrust cycle. Tide gauge data can also be used to study ETS in other places where GPS and seismic data do not exist.

2.3. Data Processing and Analysis

Hourly data from 4 NOAA permanent tide gauges (Figure 2.1.) in the Strait of Juan de Fuca and Puget Sound are analyzed to produce an estimate of the uplift at each site for each of 12 ETS events in Northern Cascadia for the period from 1996 to 2011(see Appendix C for dates).

Vertical surface displacements during an ETS event are expected to be on the order of a few millimeters over ~ 16 days. The corresponding water level changes will have the same magnitude and duration but opposite sign (because the ocean's surface goes down relative to the tide gauge when the land goes up). The level of the ocean's surface at these locations has a tidal range of 3 to 4 meters; so in order to discern an uplift signal of a few millimeters in tidal records an incredibly small signal to noise ratio must be overcome. This requires the removal of the tides, and ocean and atmospheric noise on multiple timescales, from storms that last days to decadal

8
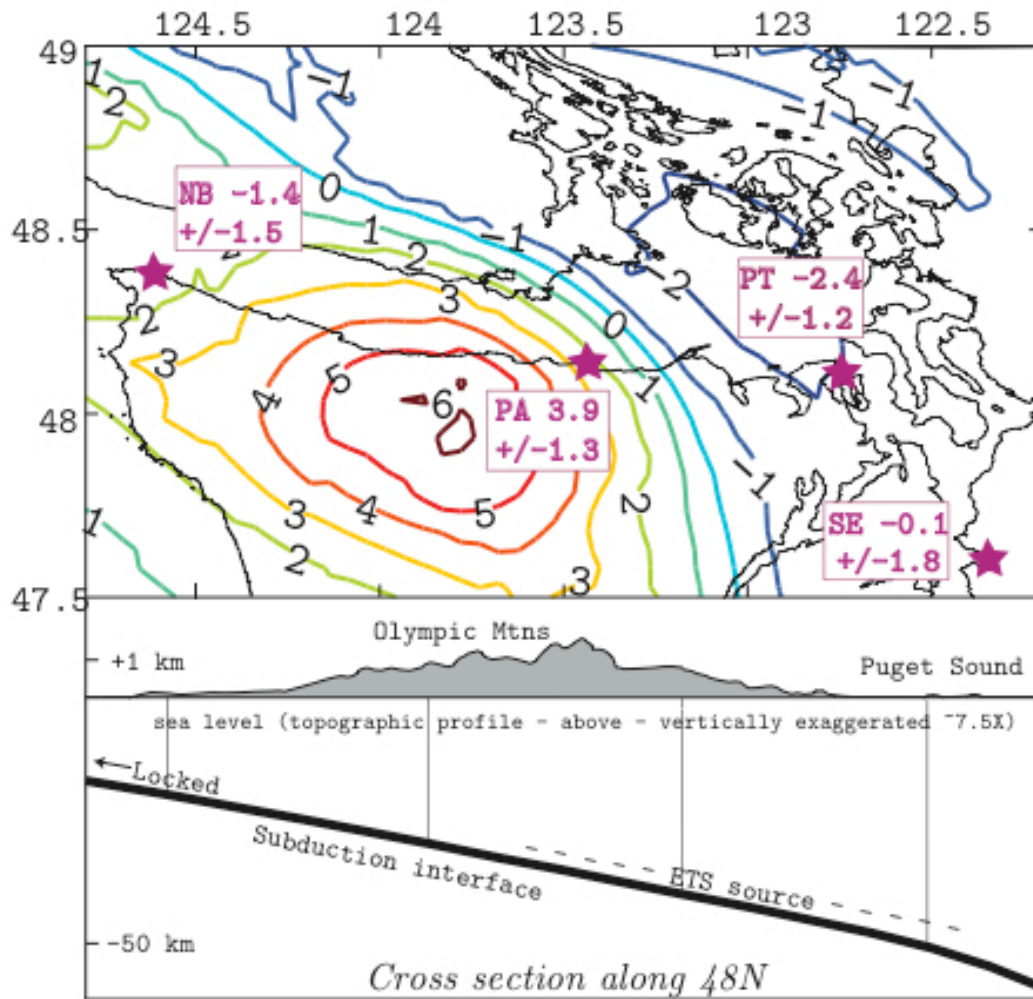
FIGURE 2.1. Top: Average uplift during ETS in northern Washington. Uplift contours are from GPS estimates of average vertical displacements for 11 events (1998-2010) estimated from modeling GPS displacements. Stars are located at 4 NOAA tide gauges (west to east: Neah Bay, Port Angeles, Port Townsend, Seattle) with 12 event (1997-2010) average uplifts with uncertainties from tidal records in bold. Bottom: Illustrated cross section along $48°N$ parallel. Updip is the locked portion of the plate which will be the source of megathrust rupture. The downdip extent of slip during a megathrust earthquake may be defined by the location of ETS along the fault.

oscillations between ocean basins. The four sites are close enough to be subject to many of the same sources of noise, yet are far enough away to have very different uplift during ETS. The fact that the tidal records have coherent noise but incoherent uplift is used to filter noise which has periods of days to weeks, without effecting the uplift signal.

First, NOAA hourly harmonic tidal predictions for each site are used to remove tides before processing. Shared residual tidal and ocean noise are then removed (Figure 2.2.) using two different methods for comparison. The two methods, described in the methods section and in greater detail in the supplementary material, are a wavelet based method, which utilizes the Discrete Wavelet Transform to compare, scale, and remove shared noise at individual time scales directly in the temporal domain, and a method that uses a frequency domain transfer function to remove coherent noise at certain frequencies. Other methods for removing noise were considered before settling on these two, including aggressive band pass filtering of frequencies representing storm noise. ETS events last days to weeks, just like storms, so have a similar frequency content. Approaches which allowed removal only of shared noise were therefore chosen in favor of those which relied on broader and more general filtering methods. The differential uplift estimated using these two distinct methods are compared for consistency and efficacy in Chapter IV. Finally, a best estimate and uncertainties of uplift or subsidence for each individual site is calculated by a least squares approach using all site differences derived from both the Transfer Function approach and the Wavelet approach.
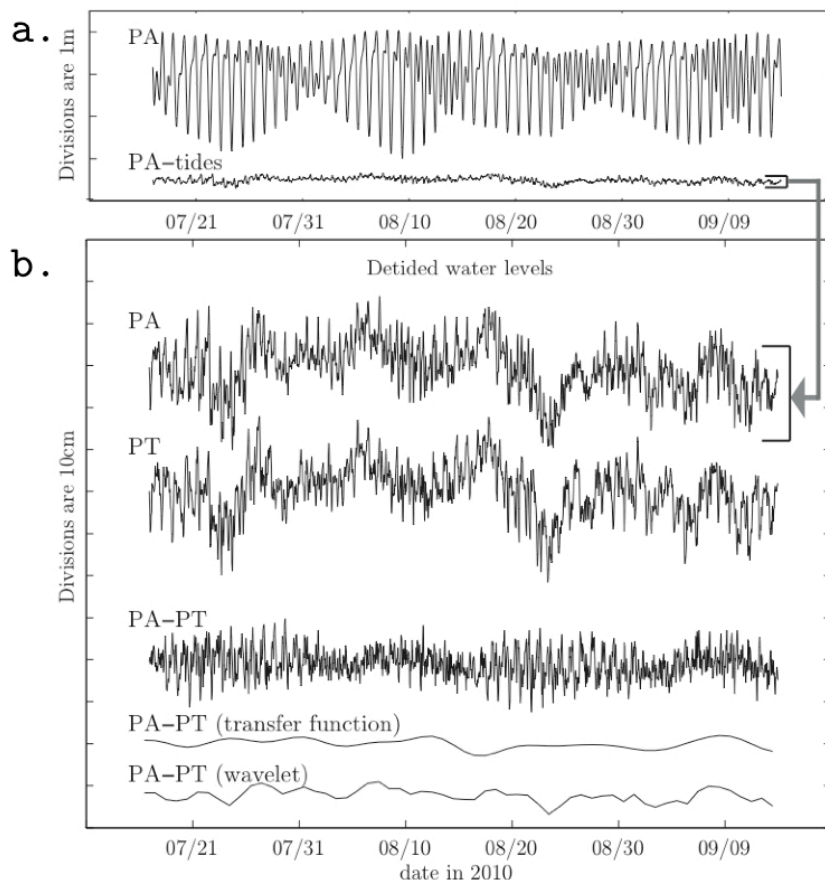
FIGURE 2.2. **a**. Water levels during the 2 months surrounding the August $5^{th} - 24^{th}$, 2010 ETS event. The top trace is hourly water levels from the NOAA tidal station at Port Angeles, WA. The lower trace is the residual series after subtracting NOAA tidal predictions. Tidal signal accounts for more than 90% of the noise in raw water level data. **b**. The top two time series are residuals following the removal of tides from Port Angeles and Port Townsend, respectively. The first is the same as the bottom trace in **a** (Port Angeles, WA) but divisions are 10 cm rather than a meter. The variations in each residual are very similar on multiple time scales. The third trace is Port Angeles less Port Townsend (after removal of tides). Closely located sites share noise which is largely eliminated simply by comparing sites in this pairwise fashion. However, residual noise still obscures uplift signals. The bottom two traces are Port Angeles–Port Townsend relative water levels after daily averaging and denoising by a transfer function in the frequency domain and by discrete wavelet transform (in the time domain).

11

TABLE 2.1. Average uplift inferred from water levels. 'Avg. Event Uplift' is the average uplift per event for 12 ETS events (1997-2010). The 'Event Uplift Rate' is the average uplift *per year*, calculated by averaging the total uplift from 12 events over 15 years of tidal records. 'Long Term Uplift Rates' are assumed to be tectonic uplifts from locking on the subduction zone. 'Inter-event Uplift Rates' are uplift rates between events when the long term tectonic uplifts are removed. Inter-event uplift rates and Event uplift rates are equal (within the uncertainty) for all sites except Neah Bay, suggesting there is strain accumulation and release in the region of ETS throughout the ETS cycle.

Site	Avg. Event Uplift(mm)	Event Uplift Rate[**]	Long Term[*] Uplift Rate[**]	Inter-event Uplift Rate[**]
Neah Bay	-1.35 ± 1.50	-1.10	3.80	1.64 ± 2.10
Port Angeles	3.86 ± 1.29	3.16	1.60	-3.19 ± 2.15
Port Townsend	-2.38 ± 1.22	-1.95	-0.20	3.08 ± 2.05
Seattle	-0.13 ± 1.78	-0.11	-0.10	-2.41 ± 2.02

[*] Long term uplift rate is from long term leveling and tide gauge data.
[**] Uplift Rates are millimeters per year.

2.4. Results

With our current processing and noise reduction the signal for individual events is usually too small to resolve absolute uplift with precision greater than the remaining noise, but the relative uplift between nearby site pairs can be resolved fro the largest events. By stacking multiple events, the signal to noise ratio is increased to where even some of the noisier station pairs have resolvable average sea level change (see Figure 2.3.). Inferred average uplift per event is shown in Table 2.1.. Average uplift estimates are consistent with GPS model predictions for 3 out of 4 sites. Neah Bay, which is on the margin of both the GPS and tidal networks is less consistent with GPS estimates (see Figure 2.1.).

One of the limitations of our processing methods is their reliance on the similarity of noise between tidal stations. As shown in Figure 2.2., the best result is produced
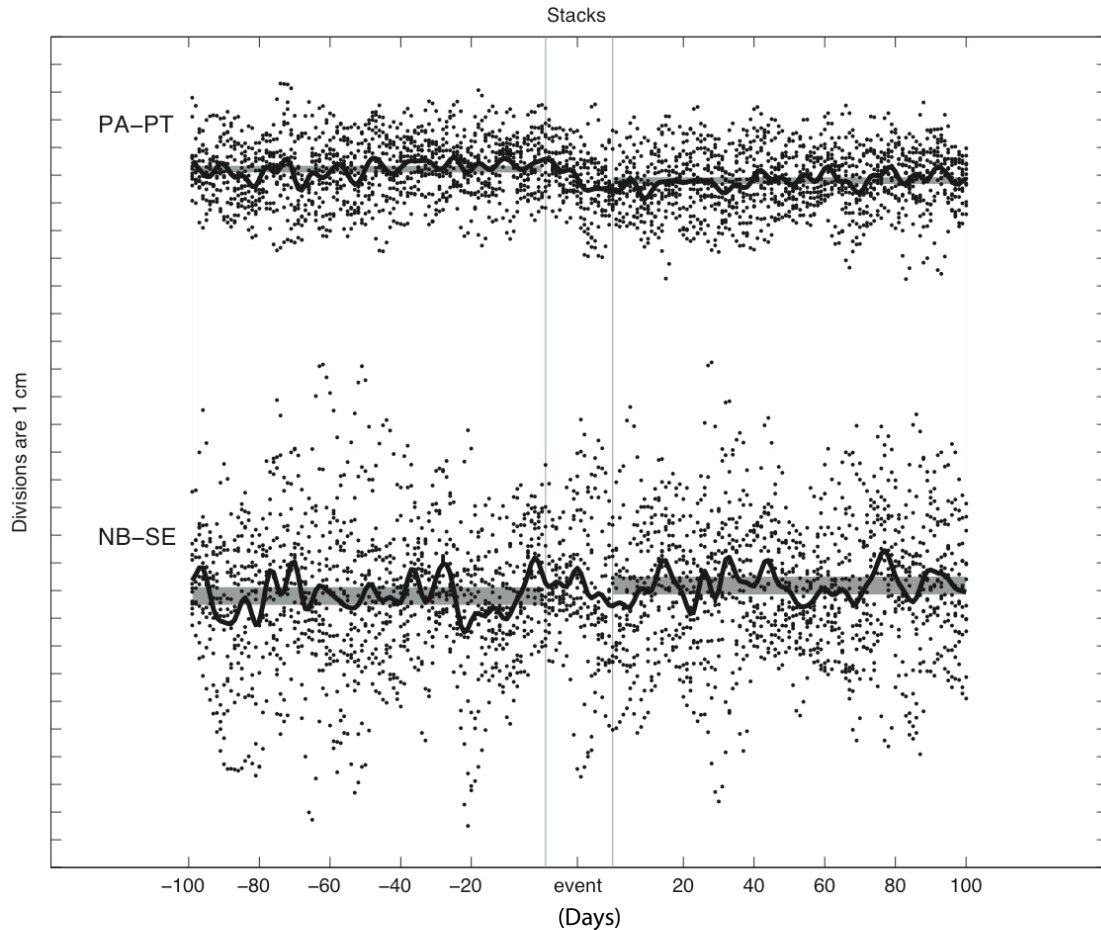
FIGURE 2.3. Average of 12 ETS events from 1997-2010. Points are individual event daily values, bold black line is the 12 event average, grey lines are centered on the means before and after the event $\pm$ the one sigma uncertainty in the mean. The top series is the best resolved and closest pair, Port Angeles minus Port Townsend; bottom is the worst resolved pair, Neah Bay minus Seattle. Average apparent water level step between Port Angeles and Port Townsend is -7.1 ± 3.02 mm (the water steps down as Port Angeles moves up relative to Port Townsend). The average step between Neah Bay and Seattle is 2.6 ± 6.1 mm. The Neah Bay-Seattle series has greatest variance due to being farthest apart as well as in disparate geographical settings (Neah Bay is very close to the open ocean, whereas Seattle is deep into the Sound), which reduces the efficacy of removal of shared noise.

13

by comparing sites in close proximity and with similar bathymetric and geographic characteristics. A comparison of Port Angeles and Port Townsend, for example, which are located close together (approximately 50 km as the fish swims) and on the south shore of the channel that forms the Straight of Juan de Fuca, results in the least noisy data series after processing. There is also a steep uplift gradient ($\sim 5\,mm$) between these two sites during an ETS event which is also an important factor in the success of this method. Pairs separated by greater distances generally have poorer resolution. Neah Bay relative to Seattle, for example, does not have a great enough noise reduction to produce a significant uplift estimate. This can be explained by the small uplift gradient between them combined with Neah Bay's distance from Seattle (more than 250 km). Neah Bay is close to the open ocean while Seattle is in the Puget Sound, producing different noise characteristics.

2.5. Interseismic Deformation

We examined rates of water level change between events to investigate the cycle of deformation, and specifically resolve vertical deformation between ETS events. The steps in water level associated with ETS are interpreted to be end-level rises (or falls, for negative values) due to tectonic uplift of the land. These are superimposed on long term sea level rise (here assumed to be $2\,mm/yr$ averaged over the 20th century [1]), long term average uplift, and uplift or subsidence that occurs between ETS events. Long term uplift rates, that span the ~ 70 years of leveling and tide gauge records, are inferred to be largely due to strain accumulation on the updip, locked portion of the megathrust interface (Figure 2.1.).To examine the uplift rates between ETS events, sea level rise, and long term uplift rates are removed. A linear regression

[1] With the interval at these gauges adjusted for shorter term variations using method of *Burgette et al.* [2009]

of combined water levels from of all the periods between events yields what we call, inter-event uplift rate in Table 2.1.. While the uncertainties are large, due to the short record and large residual noise (Figure 2.4.), on average the inter-event uplift rates are approximately equal and opposite in sign to the uplift rate that would be produced by repeated occurrence of our average ETS events.

The fact that inter-event deformation at a site is equal and opposite to deformation during ETS suggests that ETS events are, on average, releasing strain accumulated between ETS events, i.e. that ETS is consistent with the elastic rebound theory [*Reid et al.*]. While this may seem obvious given their location on the subduction interface and ETS periodicity, other physical models for ETS could be imagined, such as repeated tapping of a large reservoir of strain (perhaps built up by the last megathrust event or visoelastic effects immediately following it) modulated by the steady accumulation of pore fluid pressure released during ETS events. In the latter hypothetical case we would expect the interseismic slope to be zero, which it clearly isn't. While the current uncertainties are too large to determine whether the ETS events release all of the strain accumulated between events, our interseismic slopes strongly support the hypothesis that ETS is caused by the accumulation and release of elastic strain by a deep patch of fault on the subduction interface.

2.6. Methods

After data processing and filtering, the apparent relative water level change during an ETS event is calculated. The calculation is a simple difference of means along with a correction factor to account for possible longer term water level trends due to inter-event tectonic uplift (Figure 2.5.). To produce a difference in means, the

15
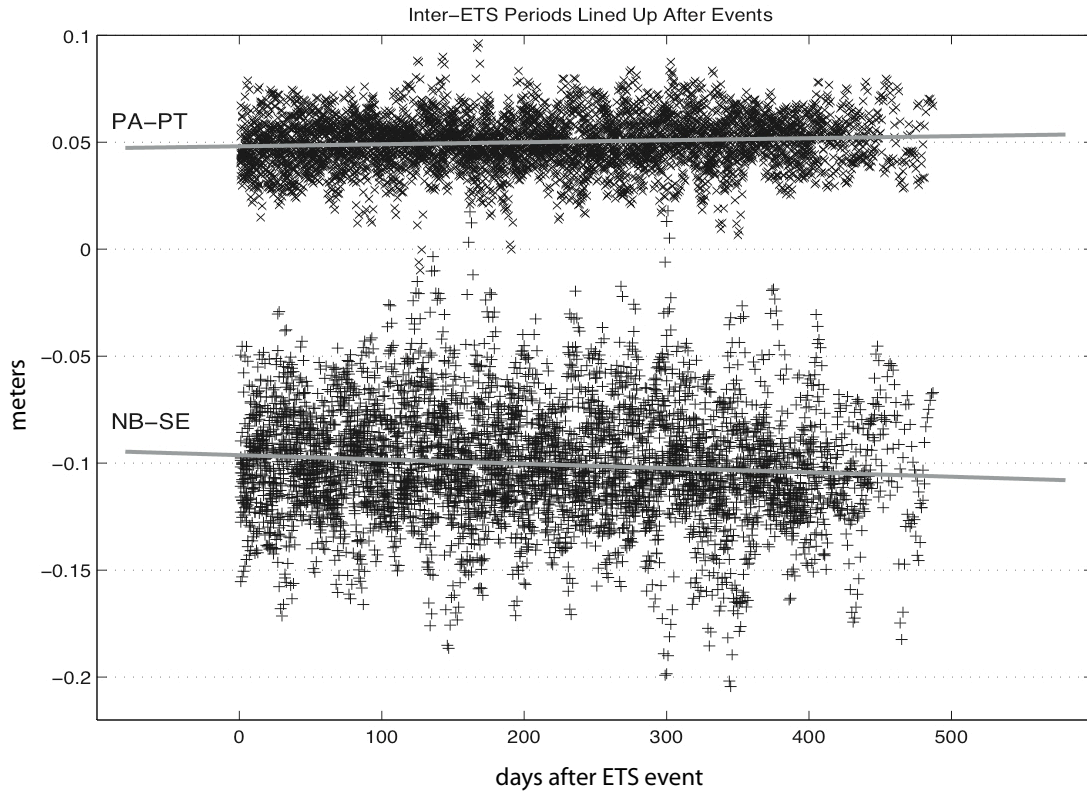
FIGURE 2.4. Transfer function denoised daily water levels from 11 inter-ETS event periods from 1997-2010 (long term trend removed). Each inter-event period was lined up on the day following the event window (10 days after the middle day of the event); data becomes sparse to the right because inter event period varies. The bold grey line is the best linear fit to the data. The top is Port Angeles relative Port Townsend, the bottom, Neah Bay relative to Seattle. The rate of relative inter-event water level slope for Port Angeles and Port Townsend is $4.5 \pm 0.5 \, \mathrm{mm/yr}$, and $-5.8 \pm 1.1 \, \mathrm{mm/yr}$ for Neah Bay relative to Seattle. As in Figure 3, the advantage of close proximity between sites can be seen in the difference in variance in the denoised water levels in the Port Angeles relative to Port Townsend versus Neah Bay relative to Seattle.

mean from the 100 days preceding the beginning[2] of the event is subtracted from the mean of the 100 days after an event. A window of 100 days was chosen to reduce the effect of high frequency noise (for further discussion see Chapter IV, Error). To correct the mean for any systematic bias produced by inter-event uplift, inter-event water level trends are calculated. Wild fluctuations in individual interseismic intervals due to climate make it impossible to directly determine slope between individual events. We use an average inter-event slope estimated by a robust regression and the mean is adjusted accordingly (Figure 2.4.).

To accurately estimate the error in the apparent relative water level change and therefore uplift during ETS, several factors must be considered. First, is the simple standard error in the estimation of the mean due to the variance in the data during an event period, denoted σ_m. Second, since the mean is corrected by the removal of the average slope of the inter-event period, the uncertainty in this correction factor, σ_c, is due to uncertainty in the regression. The third factor, and that contributing the most to the uncertainty in the apparent change is the chance of finding a random (not tectonically produced) apparent step in the water level, σ_r. Abrupt changes in water level are possible, due to meteorological changes, far field ocean processes, or gauge malfunction. To estimate the uncertainty due to randomly occurring steps, a randomly selected window of 220 days (to represent 100 days on either side of a 20 day event period) is chosen and an estimate of the step is made just as is done in estimating the apparent step for a real event. If this process is repeated many times an approximation of the distribution of randomly occurring steps emerges. The standard deviation of this distribution is taken to be the uncertainty due to the probability

---

[2]The "beginning and "end are defined as the first and last day of a 20 day window centered on the middle day of an ETS event as inferred by examining the GPS time series for Port Angeles (see Table C.1. in Appendix C for exact dates).

Idealized Step (7mm) With Noise Added

stepsize= −4.3+/− 0.21
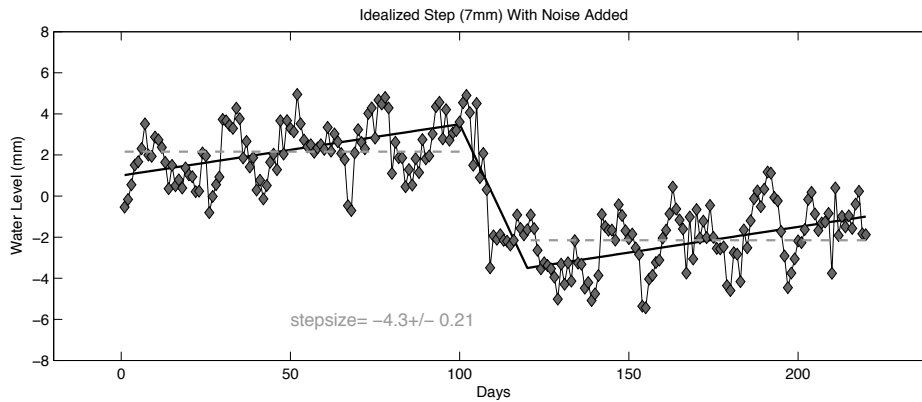
FIGURE 2.5. An idealized "event" with noise added. The black line is an idealized step in water level of 7 mm from peak to trough. The diamonds are the same idealized step with random noise and noise that approximates storms added. The noisy values are distributed about the "true water level and represent uncertainty in the mean due to variation from noise. The dashed grey line is the 100 day mean on either side of the event. The step size from a 100 day window that is required to average out the ocean noise is estimated to be −4.3 mm by a simple difference in means, which is much lower than the 'true' step of −7 mm. By estimating the inter-event uplift rate independently and adjusting the calculated step accordingly we correct for this systematic difference without biasing the interseismic slope by the step size and vice versa. We use a 100 day window to smooth out dominant periods of ocean noise. However, if there is a slope between events, as our analysis of interseismic period, on average, suggests, the step will be biased; so we adjust the steps and add appropriate additional uncertainty.

18
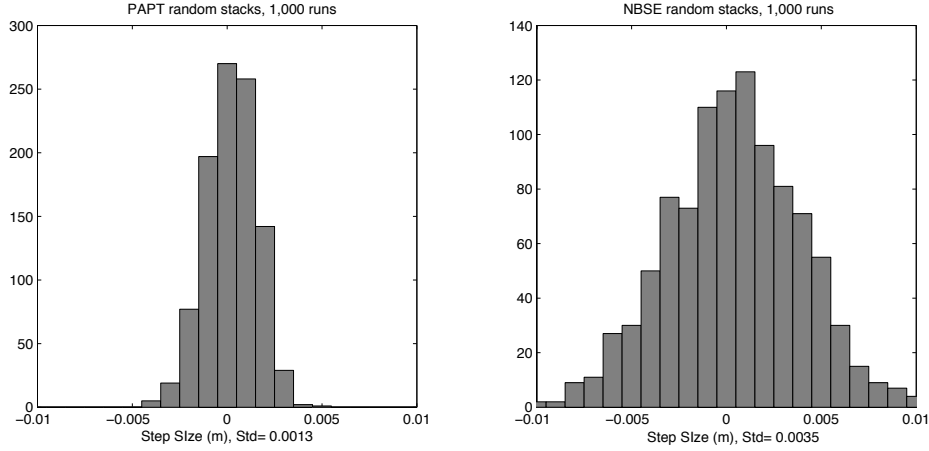
FIGURE 2.6. Distribution of randomly (not tectonically produced) steps in Port Angeles relative to Port Townsend (left) and Neah Bay relative to Seattle (right) data series. An estimate of the step size is made for a window of 220 days (100 days on either side of a 20 day "event") with a randomly selected start day. This process is repeated 1,000 times to get an approximation of the size distribution of randomly occuring steps. The standard deviation of this distribution is taken to be the uncertainty due to the probability of finding a random step in any window of data.

of finding a random step in the water level record (see Figure 2.6.). The errors are assumed to be independent and are added in quadrature to get the total error in the estimated step.

$$\sigma_t = \sqrt{\sigma_m^2 + \sigma_r^2 + \sigma_c^2} \qquad \text{(Equation 2.1.)}$$

To estimate average uplift at individual stations from multiple relative water level changes between pairs of stations we have used a weighted a least squares inversion. The inversion constrained by relative (between sites) step size estimates from transfer function denoised and wavelet denoised pairs to get an estimate of uplift at a single site [*Wolf and Ghilani*, 2002]. Also included as a constraint was the water level change at each individual station relative to a regional average. Weights, w, were calculated using the total standard error, σ_t, of each constraining factor as $w = \sigma_t^{-2}$.

19

CHAPTER III

DATA ANALYSIS

The location and magnitude of ETS events from slip patch inversions of GPS and vertical component GPS observations suggest vertical displacements during an ETS event on the order of a few millimeters over ~ 16 days [*Szeliga et al.*, 2008]. Corresponding water level drops will have the same magnitude (but opposite sign) and duration. The tidal range at a location can be upwards of several meters, which is three orders of magnitude greater than the ETS coseismic deformation. Our analyses thus require the removal of tides, and ocean noise on multiple time scales from storms to decadal oscillations. Fortunately, the four sites I consider are located proximally and therefore largely subject to the same sources of noise, whereas the coseismic uplift gradient is steep enough between sites that they have very different uplift during an ETS event (Figure 2.1.). This fact allows us to remove shared noise with frequency content similar to the ETS event while leaving the event-related uplift signal largely intact.

The first step in the analysis process is to remove the tides and bad data from the hourly water levels. The water level range can be as much as 3.5 meter between high and low tide, a full 3 orders of magnitude above the surface displacements seen during ETS (Figure 3.1.). Removal of tides by subtracting NOAA tidal predictions reveals time periods of bad data that are generally impossible to see until the tides are removed. They are fixed if the cause of the problem is obvious(Figure 3.2.). Areas of bad data which do not have an obvious cause and solution are replaced by an average of the 3 other sites.
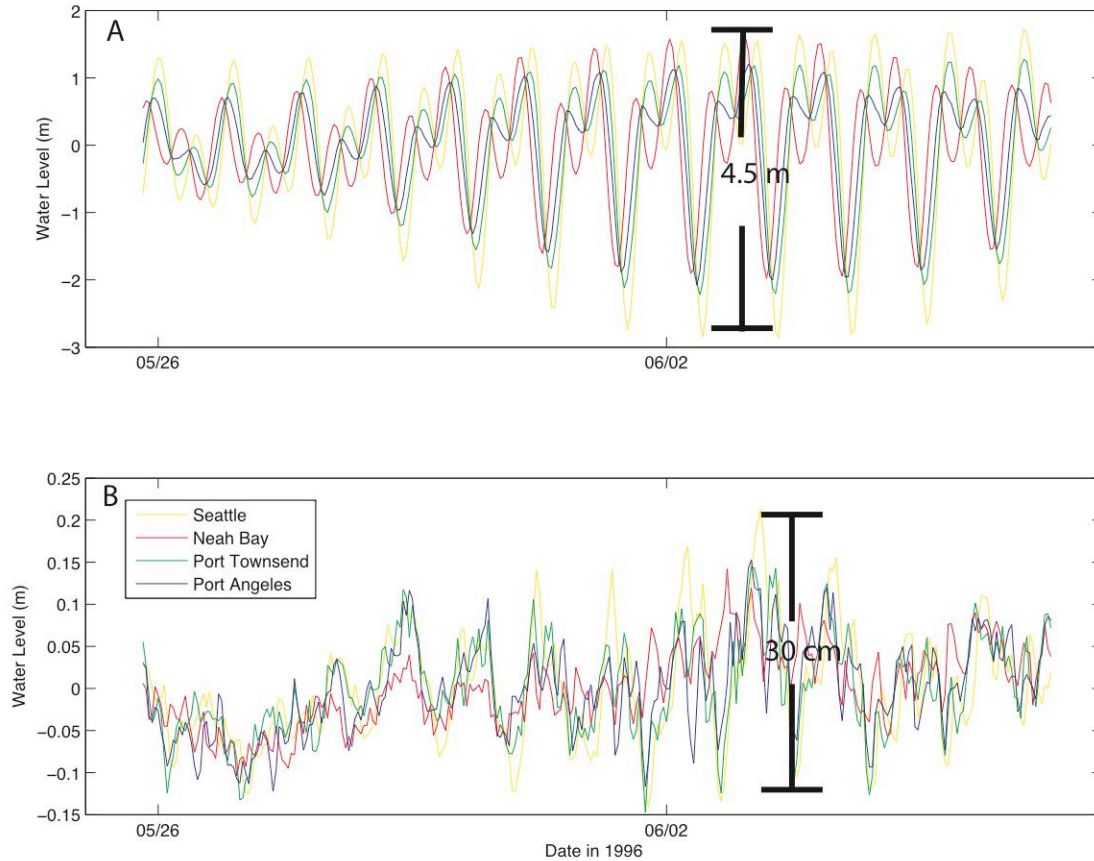
FIGURE 3.1. A) Hourly water levels at four NOAA tide gauges. The annual tidal range is over 4.5 meters. B) Hourly water levels after detiding by subtracting NOAA tidal predictions. The water level fluctuation is reduced by more than an order of magnitude. This is still 2 orders of magnitude greater than the vertical displacements during an ETS event inferred from GPS. However, the remaining noise is relatively coherent in all 4 tide gauge records, and this fact can be used to further reduce the noise level. Transfer function and wavelet denoising techniques can correlate and remove much of the noise by taking into account much of the variation in the amplitude, phase, and character of residual noise. While Port Angeles and Port Townsend (blue and green) are extremely similar, Neah Bay (red) and Seattle (orange) are not as alike (either to the first two or each other).

21
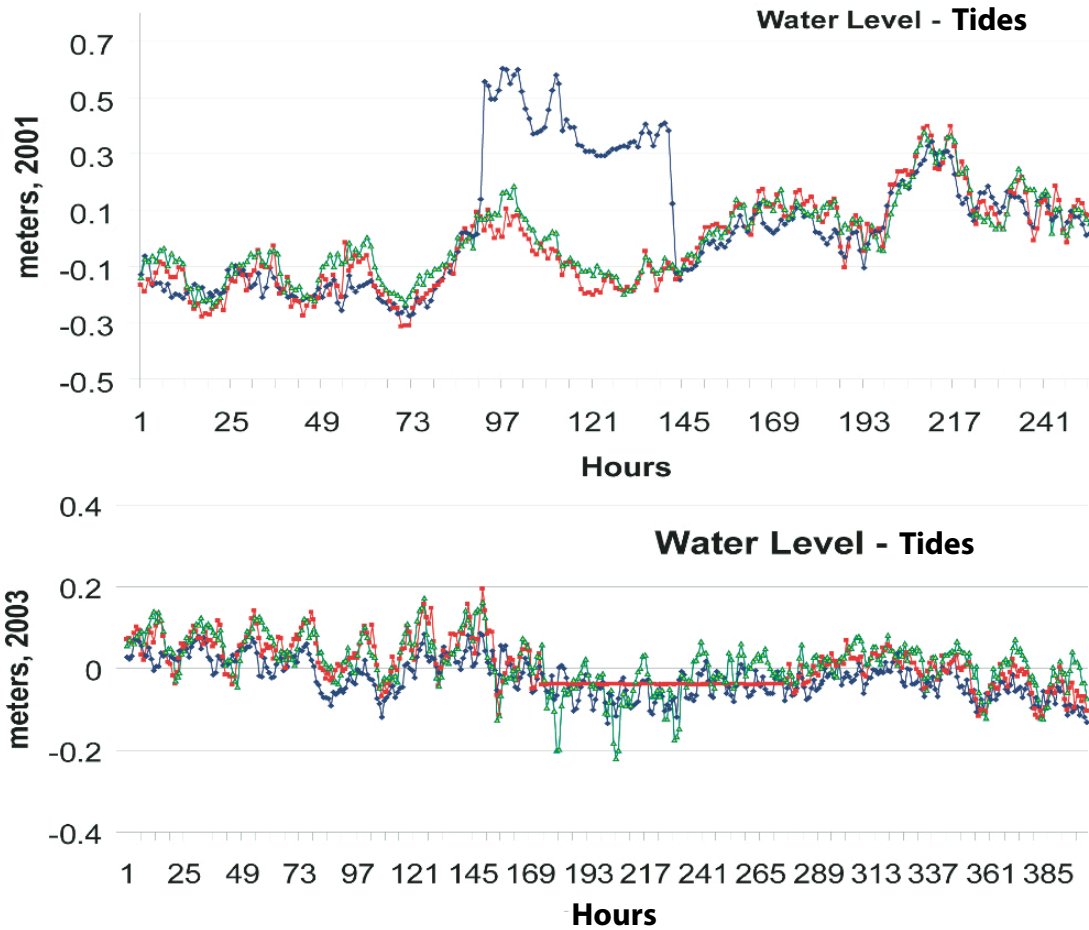
FIGURE 3.2. NOAA's "verified" data have quite a few errors that can't be easily seen until the data are detided. These errors must be corrected before one can apply our transfer function approach. The top plot is an example of a section of data from Port Townsend (blue) which has clearly been offset by 0.4 meter. In some cases, as shown in the bottom plot, NOAA has apparently put tidal predictions in the place of actual water level measurements for sections which are missing. Subtracting the NOAA tidal predictions from "real" water levels these replaced produces flat lines. The missing Port Angeles (green) water levels are replaced by an average of the other three. Neah Bay is shown in red, Seattle is not shown.

The next step in data processing is removal of shared noise with periods similar to the duration of an ETS event (Figure 3.1.). Noise with a frequency content similar to the ETS events themselves cannot simply be filtered or suppressed without removing some of the signal of interest. Two different methods to remove noise shared between sites (while preserving the difference in uplift between sites) are described here. The resultant data sets are compared in Chapter IV, both to assess which is the more efficacious method and as a means of corroborating our resultant uplift estimates for each technique. The two methods, described in detail below, are a wavelet-based method, which removes noise common to all 4 sites, at individual time scales, directly in the temporal domain, and a method that uses a frequency domain transfer function to remove coherent noise at a range of frequencies between site pairs. These denoised data sets are compared in a pairwise fashion and we use a weighted least squares adjustment [*Wolf and Ghilani*, 2002] which incorporates differential uplift estimates for each pair from both denoising methods to estimate uplift at individual sites and individual site uncertainties.

3.1. Wavelet Transform Denoising

Winter storms, regional pressure changes, and wind events all contribute significantly to what we describe as "ocean noise," and these factors are strongly shared between nearby sites. In principle this can be used to identify and remove noise, even that with spectra similar to that of ETS events; while our sites are close enough to share noise, they are far enough apart that uplift varies between sites. As a first step, a regional noise signal is created from a simple average of the subtidal residual (original time series minus predicted tides) at each site. In general, during an ETS event, some sites go up and some go down, so that the

uplift signals tend to cancel each other out making the regional average uplift for any ETS event approximately zero. Bathymetric and geographic differences between stations enhance or diminish noise within certain frequency ranges for a particular site, however, which precludes subtracting a very simple scaled average of the regional noise signal. To account for differences in the noise spectra between sites, we use a Discrete Wavelet Transform (which I will refer to as the "wavelet approach" to distinguish it from the "transfer function approach" discussed below) to decompose the regional noise signal into "details" at different timescales and scale the regional noise at each detail to an individual site (Figure 3.3.). The scaling is done by a simple linear fit of the individual site values for a detail to the regional noise signal at the same detail level (Figure 3.4.). The first wavelet detail has noise with a timescale of ~ 3 days, and the average timescale doubles for each increasing detail. A Daubechies No. 7 mother wavelet (Figure 3.5.) was chosen because it resembles a water wave [*Goring*, 2008] and has periods (wavelength of the central peak and trough)[1] roughly equal to convenient temporal quantities (for example, detail level 8 has a period equal to ~ 370 days which is very close to one year). Details up to detail number 10 are considered, corresponding to average timescales of approximately 3 days to 4 years. After the noise signal is scaled at each detail level, they are combined to make a scaled regional signal specific to that site which is subtracted from the original record, thereby denoising it.

3.2. Transfer Function Denoising

Noise can also be removed in the frequency domain. After taking the Fourier transform of two water level records we estimate a transfer function between the

---

[1]For further explanation of wavelet periods see MATLAB wavelet toolbox scal2frq function reference in the MATLAB Wavelet Toolbox User's Guide [*Misiti et al.*, 1997]
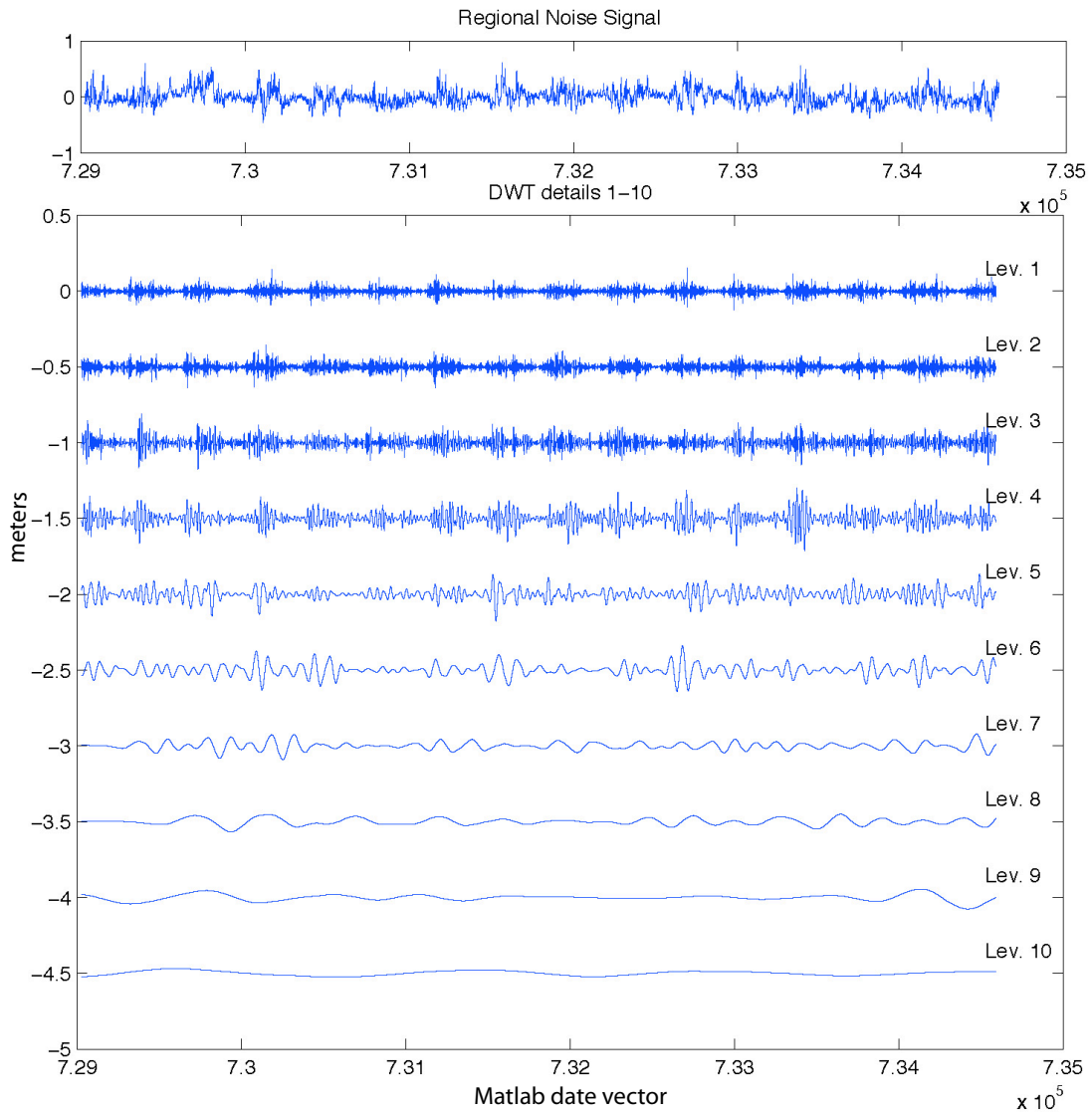
FIGURE 3.3. Top is the regional average noise signal made by average all 4 stations' time series'. Below it are the Discrete Wavelet Tranform (DWT) decomposition of the regional noise series at each detail level from 1 to 10. Detail 1 at the top corresponds roughly to noise with a period of 3 days, this is doubled at each detail level, so that level two is ∼ 6 days, level 3 is ∼ 12 days, and so on. A linear combination of the details reproduces the original signal.
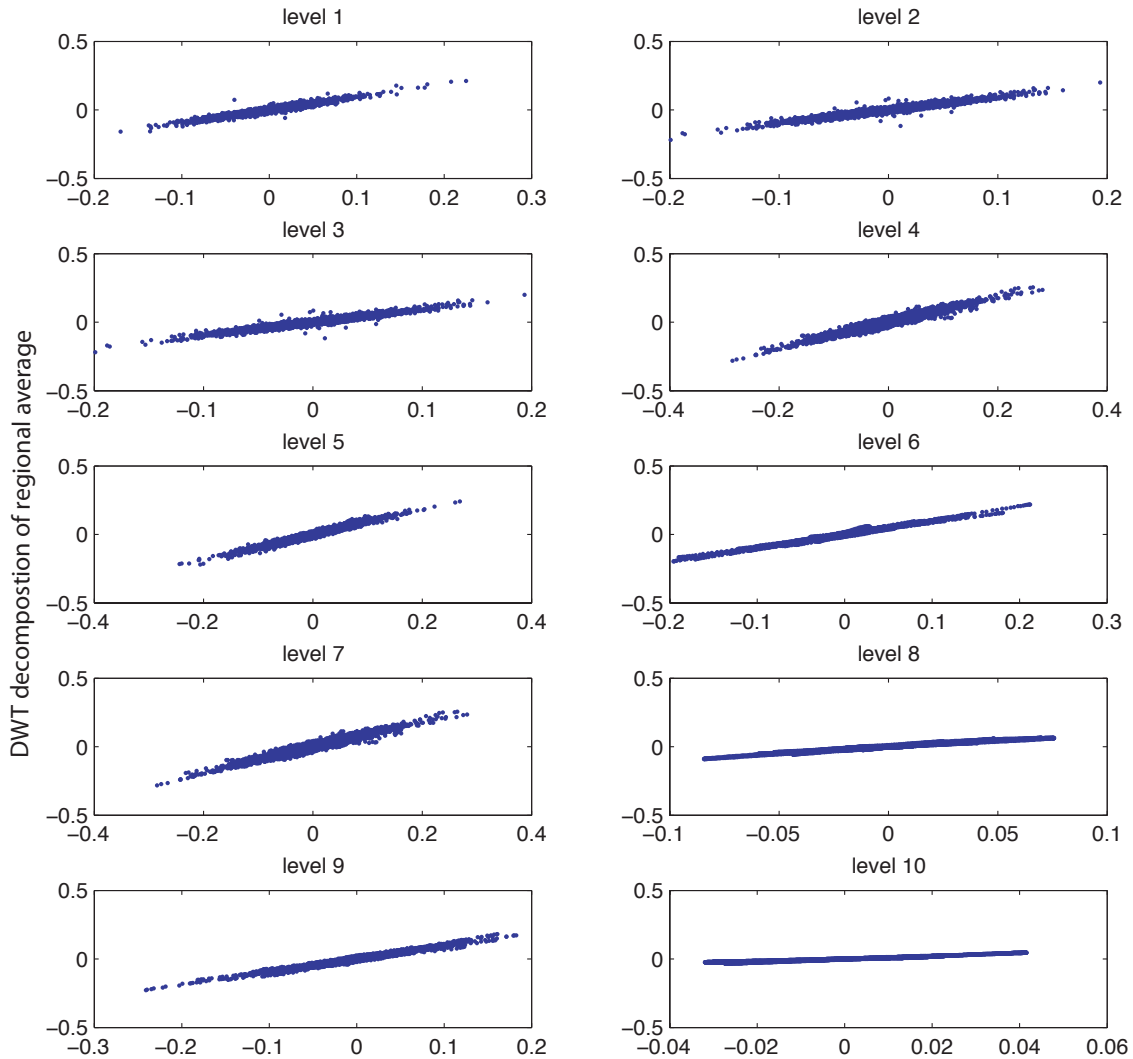
FIGURE 3.4. Scaling of Port Townsend (y axis) to the regional noise (x axis) at each DWT decomposition detail level. Each site is decomposed and compared to the regional average time series at each detail level in order to scale the regional average for that site. The scaling accounts for different amplitude response to noise at different timescales which are unique to a site. After the scaling, the details are recombined to create a scaled estimate of noise shared between all 4 sites which can be subtracted from the series.
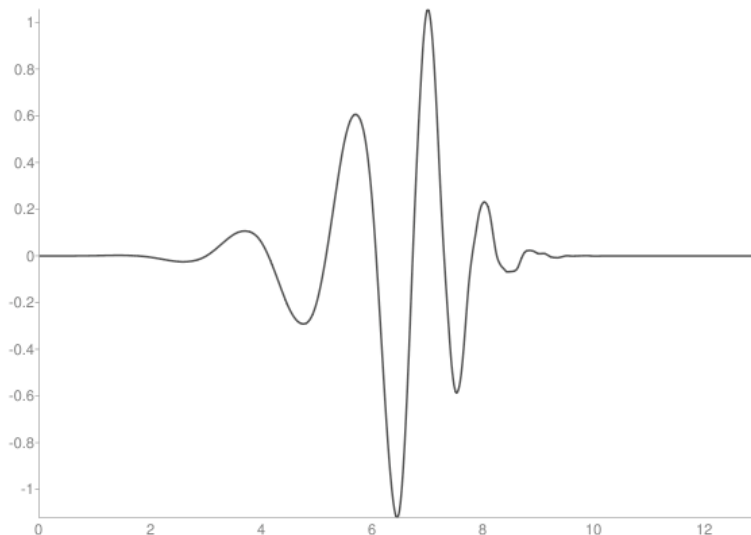
FIGURE 3.5. Daubechies No. 7 mother wavelet.

spectra of the two sites (Figure 3.6.) in a moving window. We can apply the transfer function to the Fourier transform of the second time series to get an estimate of the first time series in frequency space [*Wei*, 1994]. By limiting the window size we filter only noise with periods of weeks to months. Since we are only interested in filtering out shared noise, we do a cross correlation in the frequency domain (Figure 3.7.) to determine at which frequencies the two time series' are coherent [*Krauss et al.*, 1994]. We then apply a coherence mask which deemphasizes those frequencies at which the two sites are incoherent or which are outside the frequency range of interest. We then apply an inverse Fourier Transform to the noise estimate to give us back an hourly time series which is essentially an approximation of the shared noise only at those frequencies we desire in a window of data. We slide the window and build a continuous time series of shared noise by averaging the overlapping windows. This time series can be subtracted from the data set at the first site. The result is the water level time series at the first site, less any coherent noise shared with the second site. The transfer function approach allows us to remove noise with slightly different

27

amplitude and phase but the same frequency, and we have to define how different we allow noise to be before it is incoherent. We tend to be conservative in defining "coherent" because the lower the cutoff for "coherence" (the greater the difference between noise we consider "the same"), the greater the possibility that some of the non-coherent ETS signal will be removed as part of the process. As mentioned above, denoising relies on the assumption that noise is shared between sites while uplift is not. If two sites have uplift with the same sign, but different amplitude, the differential uplift might still be substantial, but denoising by the transfer function approach may remove some of the uplift signal because the frequency character of the uplift is similar even though the amplitude is very different. To minimize any artifacts produced by the transfer function process and any deleterious effect on the uplift signal which might result from denoising a site by a site that has a somewhat similar uplift signal, each site is denoised by all three other sites and a denoised site average is made by combining all three.

3.3. After Denoising

The uplift signal is usually still below the noise at a single site, even after the removal of tides, and ocean noise. However, it is often the case that the two sites being compared will have uplift of opposite signs, so that the differential uplift will be greater than the uplift at an individual site. A comparison of water levels at sites in a pairwise fashion is thus employed to amplify the signal, while often simultaneously removing residual shared noise (Figure 3.8.). To do this, we subtract one site from another (they are compared in such a way as to always get a negative water level step during an event).

28
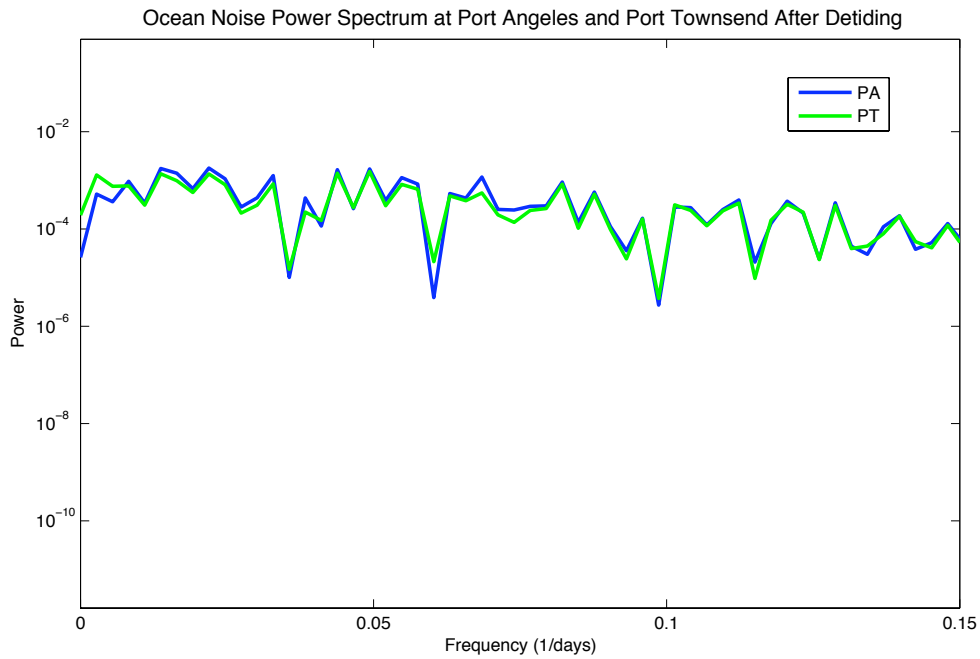
FIGURE 3.6. Power spectrum of Port Angeles (blue) and Port Townsend (green). The frequency composition of both data sets is very similar as would be expected from their proximity. To denoise Port Angeles, unshared frequency components can be masked in the frequency domain. When we estimate a transfer function only coherent frequencies are represented so that an inverse Fourier transform of the output of the transfer function gives us an approximated shared noise signal in the time domain which can then be subtracted from the original detided series.
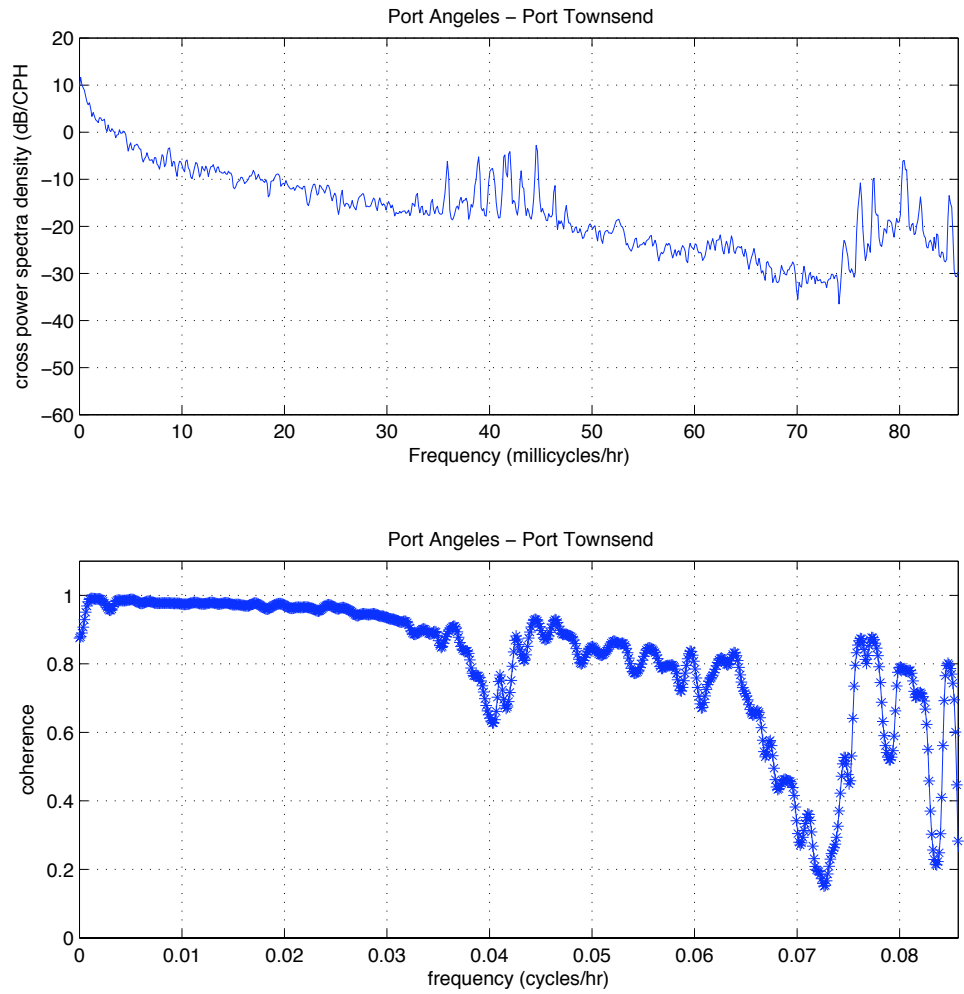
FIGURE 3.7. Coherence and power spectra of Port Angeles and Port Townsend. The top figure is the cross power spectral density of Port Angeles and Port Townsend. It tells us which frequencies have the greatest noise shared between the two data sets. The bottom is the coherence between the two time series at different frequencies. All frequencies with a coherence level below .5 are masked out before applying the transfer function ensuring any unshared signal is not removed from either site's time series
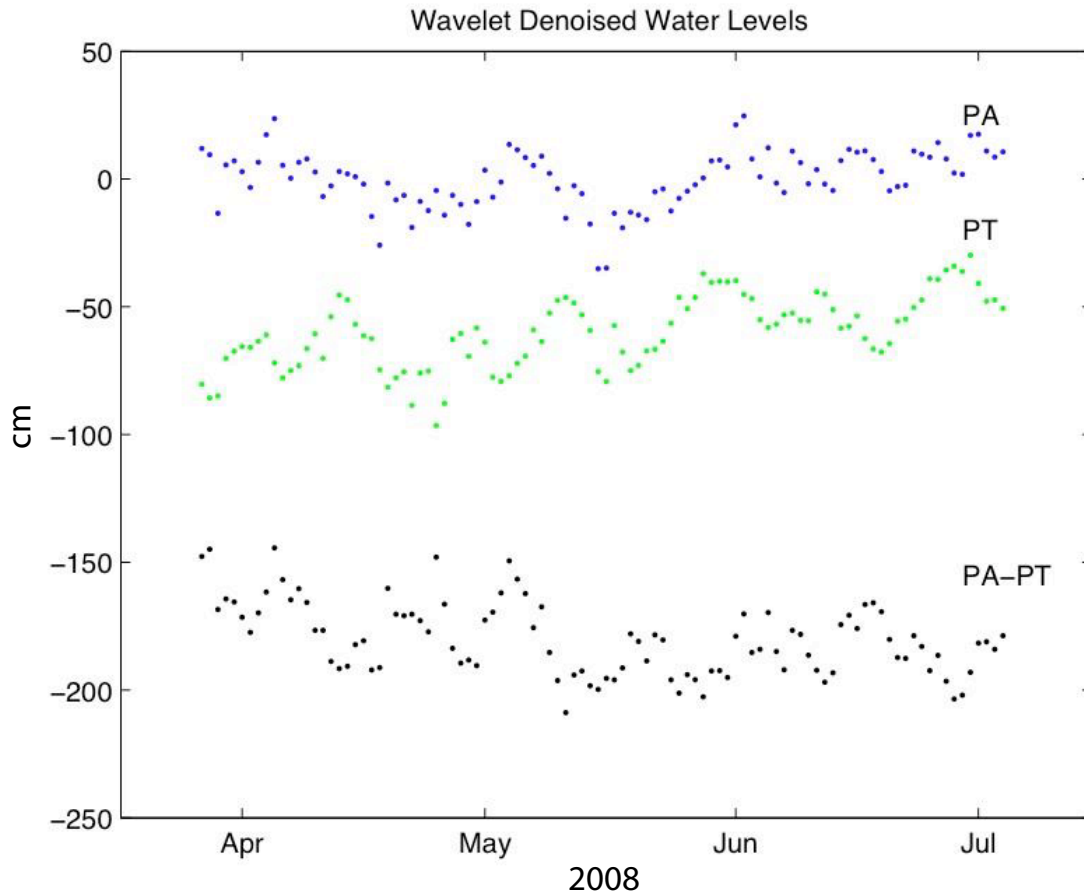
FIGURE 3.8. The top two series are the Port Angeles and Port Townsend daily water levels in mm for the May 2008 ETS event. The amplitude of the remaining noise in the individual series is several cm, obscuring the small (several mm) uplift signal. By subtracting Port Townsend from Port Angeles the long period noise is reduced whereas the uplift signal we are looking for is enhanced because, in general, Port Townsend goes down and Port Angeles goes up during an ETS event. So the uplift becomes visible in the plot of Port Angeles relative to Port Townsend (lower).

31

Denoising with either approach and pairwise differencing does not remove residual seasonal cycle differences between sites or differences in site response to decadal ocean basin oscillations so that denoised differential time series' still have considerable long period noise. An attempt was made to estimate the average differential seasonal cycle for each site pair by averaging monthly mean water levels for all the years of data. However, the magnitude and phase differences were very large between years and no satisfactory method was found to remove seasonal variations. Lastly, to remove differential response to decadal oscillations, a 460 day running average of each site pair is subtracted (a 460 day average does not remove any of the ETS signal because it is greater than the average ETS periodicity).

Water level changes during individual ETS events[2] rarely exceed their estimated uncertainties. Although individual event remain obscure, we can stack the 12 event windows to get the average water level changes with greatly reduced uncertainties[3]. Chapter IV, Error, has a detailed description of uncertainty estimation and a comparison of the efficacy of both denoising methods.

---

[2]For water level step estimates and uncertainties for individual events, see Appendix A

[3]For average water level step estimates and uncertainties, see Appendix A

CHAPTER IV

ERROR

4.1. Error in the Estimation of Apparent Water Level Change

The one sigma uncertainty in the estimation of water level changes between sites has 3 components: the uncertainty in the uncertainty in the difference in the means, the probability of finding a step randomly in any pair, and the uncertainty in the inter-event slope correction factor. To get the total uncertainty in the estimation of differential apparent water level changes between sites, these three sources of error are assumed to be independent and added in quadrature. This error then goes into the ordinary least squares inversion as a weighting factor (see Appendix D).

4.1.1. Uncertainty in the Mean

As the water level at a site fluctuates due to seasonal oscillations, storms, tides, boat wakes, and all the other sources of noise, it is fluctuating about some idealized "mean sea level. For discussion, consider a simple idealized model of deformation during ETS: a linear change over sixteen days with a stable unchanging height on either side of the event extending infinitely before and after the event (Figure 4.1.). In practice, however, after removal of tidal signals and shared noise, we are still left with considerable residual noise.

Residual ocean noise, which is largely due to the site response to storms and other open ocean derived water level changes, is greatest in pairs which are not located as closely together. Building on the previous hypothetical case, if we add residual noise with periods similar to that produced by storms (approximately 3–14 days) and random white noise we would expect it to look like the bottom of Figure 4.1.. The

true water level within some window should lie within the standard deviation of a calculated mean water level. The sensitivity of the mean to the variations caused by noise (the ups and downs) is dependent on how many such excursions are included in the window used to calculate the mean. The larger the window of data the less sensitive the mean is to noise variations.

4.1.2. Probability of Finding a 'Random' Step

There is some probability of finding a random step in water levels (random in the sense that it is not due to tectonic processes). Such steps can be only apparent steps, due to instrumental error or instability in the gauge, or real abrupt changes in water levels, due to ocean processes, barometric pressure changes, or sudden introductions of large volumes of water from land based sources that are not removed by our processing. To minimize the effect of these 'random' steps on the uncertainty in our estimation of water level changes, the largest window possible should be used to calculate the mean water level on either side of the event, because the smaller the window is, the more likely we are to find a randomly occurring step.

To estimate the probability of finding a step of a certain size for a given window size, we randomly select a window of data and calculate the step size using the same procedure we would for a real event. We can do this 1000 times to get a distribution of random step sizes. To get the probability of finding a random step in a stack of 12 events, we do the same but chose 12 random windows and stack them. We then calculate the the step size for the random stack. The standard deviation of the distribution of random step sizes is the uncertainty in the step estimate due to the probability of finding a random step (Figure 4.2.).
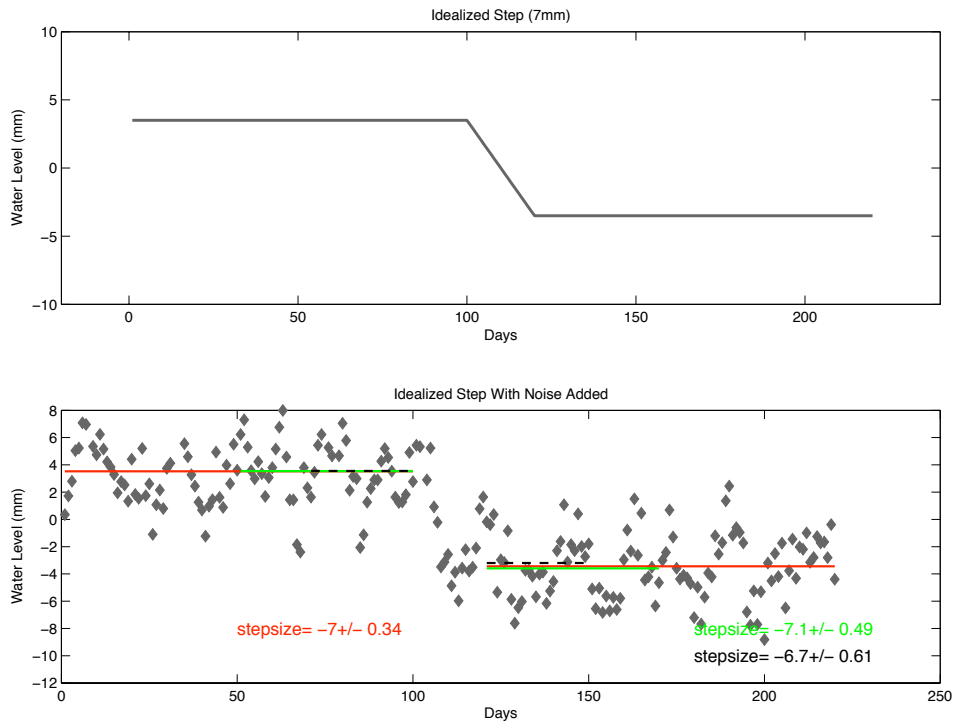
FIGURE 4.1. The top plot is an idealized water level change. It is like a stair step which a constant water level on either side of a 20 day event, with a step of −7 mm. The bottom shows the same step but with storms and random noise added. To calculate the step size we calculate a difference in means before and after the event, using different window sizes to see the effect of noise on the mean. The red lines are the 100 day mean, the green lines are the 50 day mean and the black dashed line is the 30 day mean. The storms and random noise can effect the estimated mean depending on how many positive or negative excursions are included. The more storms we include in our mean, the less effect they have, tending to average to zero
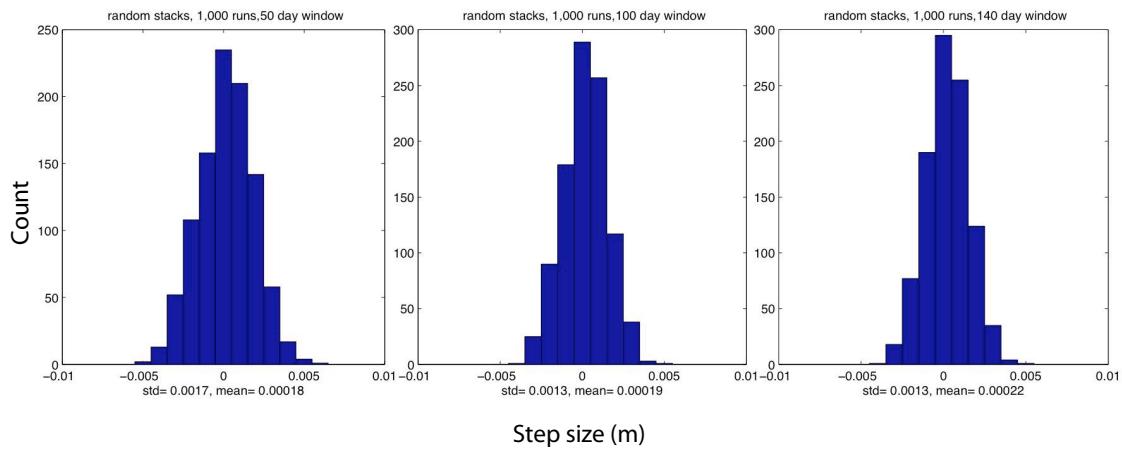
FIGURE 4.2. Distribution of step sized calculated from stacks of 12 randomly selected windows of data (Port Angeles relative to Port Townsend). This is representative of the probability of finding a step which is not tectonically produced in a stack. The histogram on the left uses as window of 50 days on either side of a 20 day event window to calculate the step size, this middle is 100 day windows on either side and the histogram on the right is a window of 140 days on either side. There is a significant reduction in the width of the distribution from 50 day windows (standard deviation is 1.7 mm) to 100 day windows (1.3 mm) but little or no advantage when going from 100 day windows to 140 day windows.

4.1.3. Uncertainty in Inter-Event Slope

The long term uplift rate combined with the average per event uplift suggest that the ETS cycle resembles a saw blade where the Earth's surface moves up and down as the slip patch accumulates and releases strain (Figure 4.3.). If we assume that the rate of inter-event strain accumulation is constant, the inter-event deformation rate (uplift or subsidence) should also be constant. The step size is underestimated by some amount each time due to averaging a window of data (Figure 4.4.) where a slope is present. This bias can be adjusted by a correction factor to account for the inter-event slope if we know the inter-event uplift rate. The uncertainty in this slope propagates through to the step size estimate.

To estimate the inter-event slope, we take each of 12 inter-event periods from 1996-2010, line them up on the day after the event (Figure 2.4.), demean them to remove very long period ocean fluctuations, and fit a line to them using the MATLAB function robustfit [*Misiti et al.*, 1997], which utilizes an iteratively reweighted least squares algorithm with a bisquare weighting function. The robustfit is preferable to the ordinary least squares algorithm to reduce the effect of outliers on the slope estimation. The robustfit function returns an array of fit statistics including the standard error of coefficient estimates. The slope is then used to calculate a correction factor (Figure 4.5.) and the the error in the slope coefficient is used to calculate the error in the correction factor.

4.2. Adding an Artificial Step

To assess the efficacy of both denoising methods, we have added an artificial 'event' of a known size into one of the data sets which simulates the inter-event and coseismic deformation of the ETS cycle. By adding a step a a known size to the data
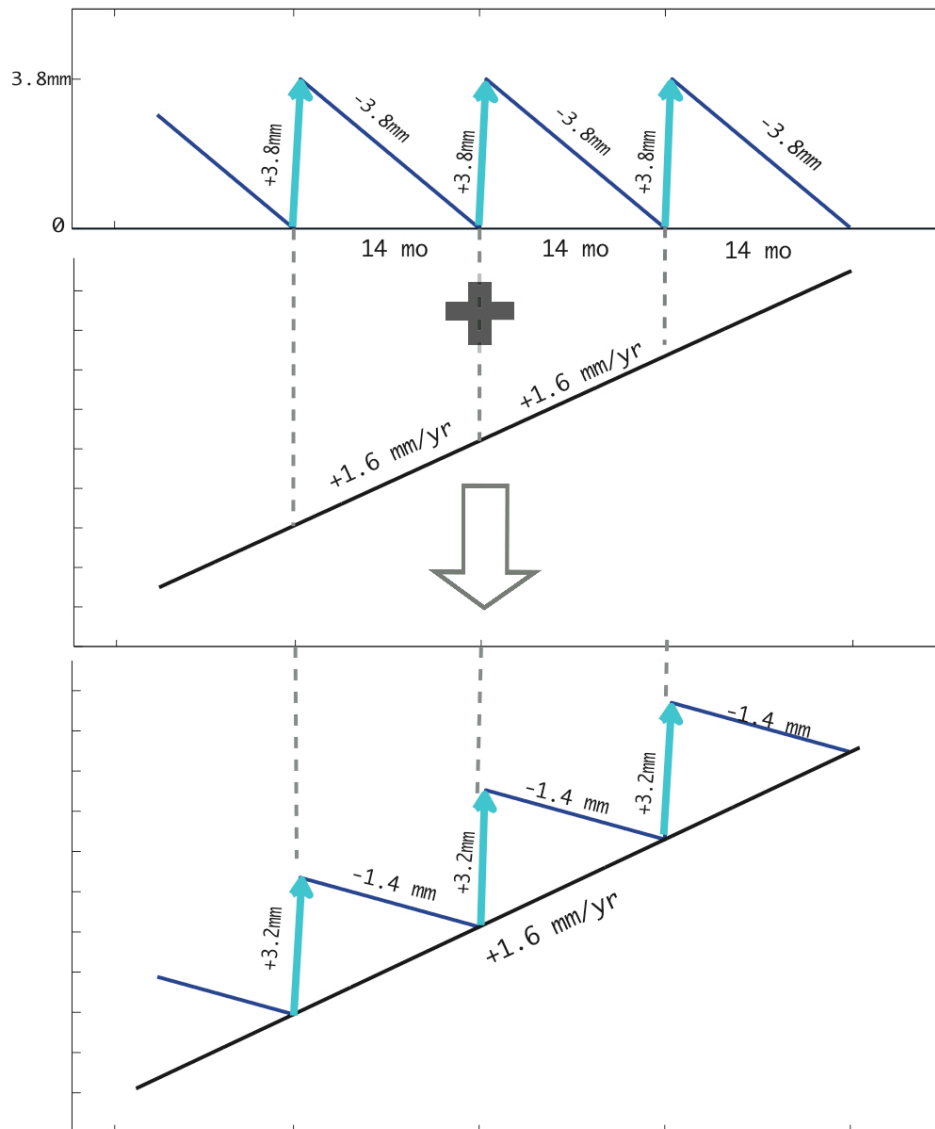
FIGURE 4.3. If we look at a hypothetical representation of differential uplift between Port Angeles and Port Townsend we find what resembles a saw blade. The ETS cycle (top) depicts the accumulation and release of elastic strain, Port Angeles goes down relative to Port Townsend during the inter-event periods and then abruptly goes up (relative to Port Townsend) during an ETS event. This cycle is superimposed on the long term uplift due to locking on the updip "locked zone" (shown in Figure 2.1. of the subduction interface (the source of megathrust earthquakes).

38
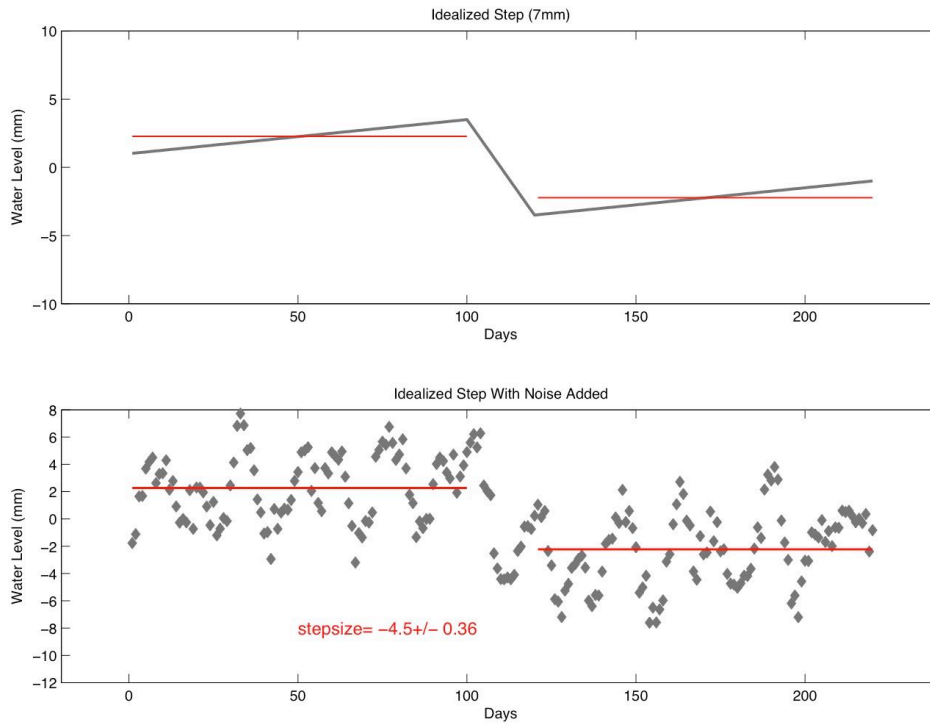
FIGURE 4.4. This is a hypothetical time series of an ETS cycle which is a saw tooth rather than a stair step. The water level gradually rises over 300 days then drops 7 mm over 20 days before again rising gradually. The bottom is the same idealized step with artificial "storms and white noise added. The red line in both is the 100 day mean water level. Because of the gradual slope of the inter-event uplift, a difference in means underestimates the step size considerably. We can adjust this to account for the inter-event deformation rate when estimating the size of real events.
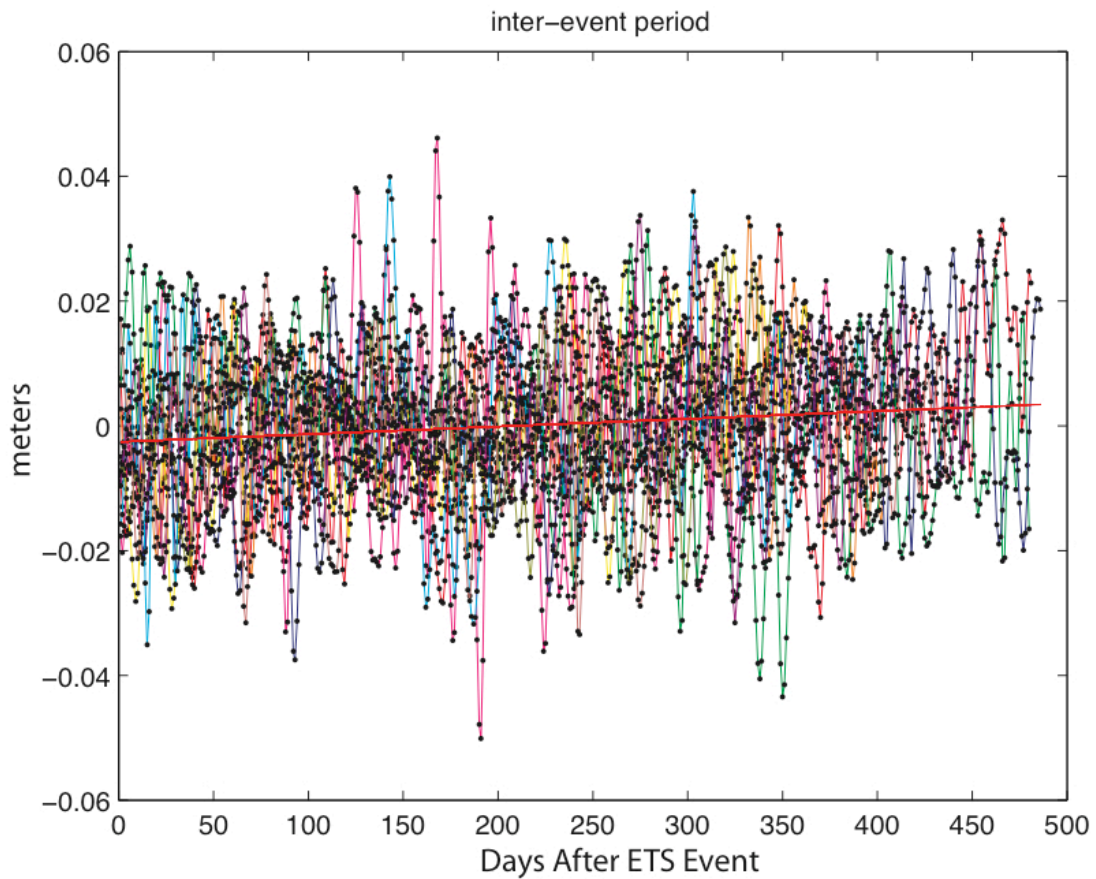
FIGURE 4.5. Black dots are the daily relative water levels for Port Angeles and Port Townsend for 13 inter-event periods from 1996–2010. The colored lines connect days in a particular inter-event period. The red line is the best fit line, in green is the slope of that line in m/yr. This inter-event slope is used to make a correction factor for step estimation and used as a constraint in the least squares approximation of inter-event uplift.
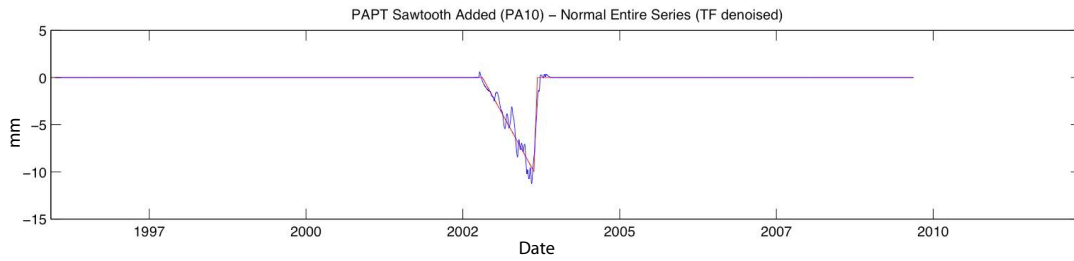
FIGURE 4.6. A gradual change over 300 days followed by and abrupt change of 10 mm over 20 days (shown in red) was added to Port Angeles. The blue trace is the original denoised Port Angeles relative to Port Townsend minus the denoised series after the artificial step was added. Although the blue trace demonstrates that transfer function denoising does not pass uncorrelated noise perfectly, the size and general shape of the artificial step is retained after denoising.

we can determine how effective our method is for estimating the step size correctly, and whether any bias is caused by denoising, for example, whether noise is added by either denoising approach or whether the magnitude and shape of the step are recovered. An artificial gradual water level decline from zero to -10 mm over 300 days, followed by an abrupt change (or step) over 20 days of 10 mm, was added to the Port Angeles tidal time series(Figure 4.6.). This adds an artificial step of a known size and location, while the water levels before and after the gradual rise and step remain unchanged.

After going through the complete processing, the result is an affirmation that, for individual events, the noise is still too great to reliably discern the step even for the largest events in Cascadia. An examination of the window of data (Port Angeles relative to Port Townsend) around the 'event' does indicate that the step size is at least retained after denoising by both the transfer function approach (Figure 4.7.) and the wavelet approach (Figure 4.8.). However, for an individual event, neither approach effectively removes noise so that the uplift can be seen. The estimated step size for the original Port Angeles relative to Port Townsend data series denoised by

the transfer function approach is $-13\,\mathrm{mm}$ (a large negative step due to residual ocean noise of some kind). The estimated step size for the same series in the same window, after adding the artificial step is $-4\,\mathrm{mm}$ (still negative, even though we have added a step of $10\,\mathrm{mm}$ to the Port Angeles). The difference between the estimated step size with and without the artificial step added, $9\,\mathrm{mm}$, approximately equals the size of the added step. By comparing the denoised pairs with and without an artificial step, we can see that the transfer function does not remove any of the signal, even if an accurate estimation of its true size is obscured by noise. The wavelet approach appears to produces a consistent result but the difference in the estimated step size before and after adding a artificial step is $8\,\mathrm{mm}$.

Though the artificial step test shows us the limitation of these processing methods for individual events, the results are also relevant to the stacks of events. When events are stacked, the error and noise are greatly reduced so that the fact that the transfer function preserves the step size means that, even though individual events are lost in the noise, we can expect to get an accurate estimation of the average step size. Another concern which is relevant to the average step size is whether our processing is the same when two sites being compared have deformation with the same sign. Since both approaches remove shared noise, it is possible that the result is affected depending on whether the individual sites being compared are "stepping" in the same direction. To test this, we add an additional step of $5\,\mathrm{mm}$ to Port Townsend (giving an overall uplift of $5\,\mathrm{mm}$ for Port Angeles relative to Port Townsend). The result is much the same as in the case when a step was added only to Port Angeles. Neither approach gives an accurate estimate of the actual step size but the step is preserved (Figure 4.9.), so that we should expect to get an accurate estimate of the average step size with the reduced noise of a stack. The wavelet approach again produces a

42
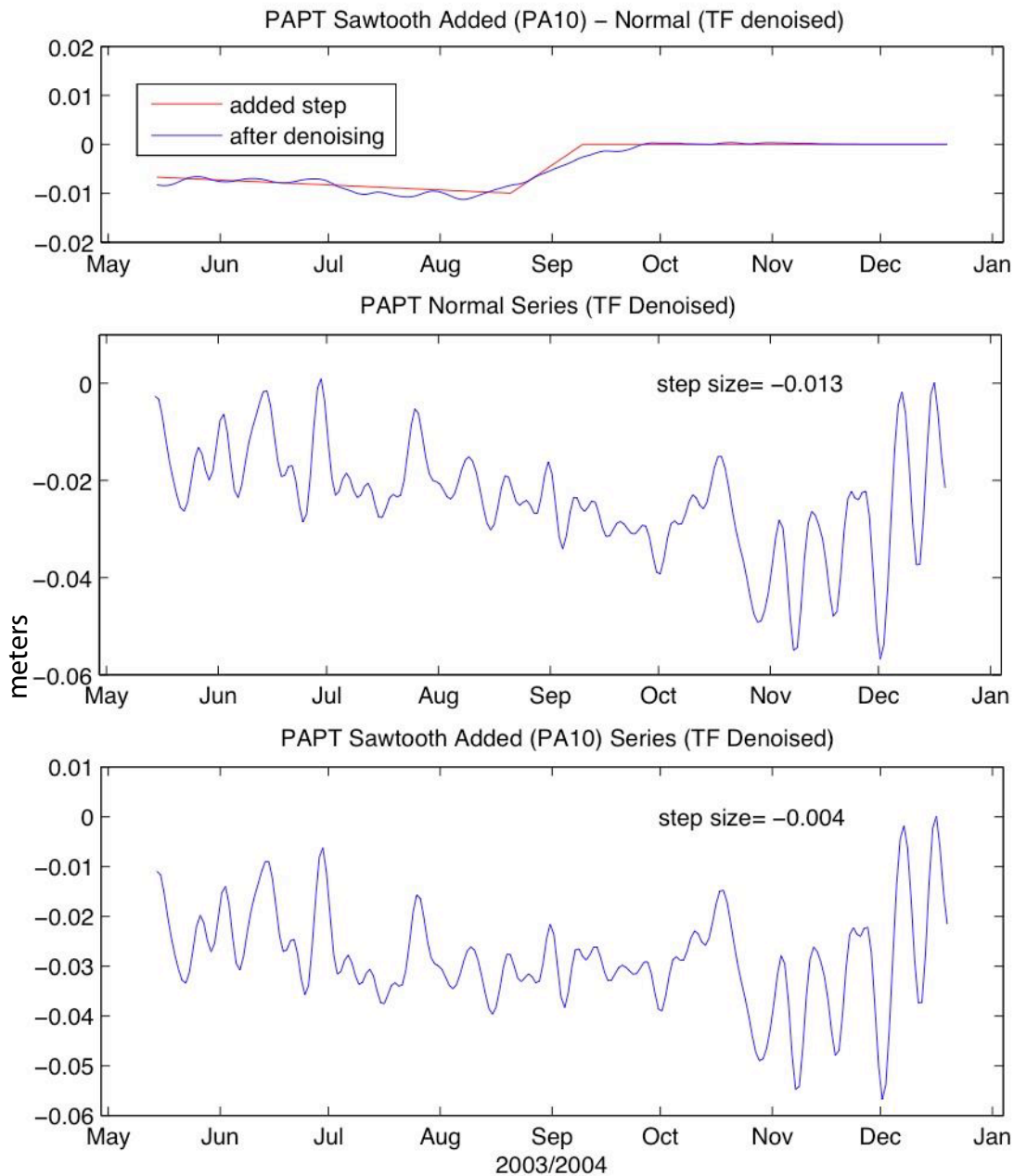
FIGURE 4.7. The top figure is a close up on the event window for the residual between the original denoised Port Angeles relative to Port Townsend series and the artificial step added denoised series. The middle plot is daily water levels during the "event" window without the added step. There happens to be a step here of −13 mm due to residual noise. In the bottom plot, which is the same window of data after denoising with an artificial step added, we see that although the estimated step size (which should be 10 mm) does not even have the correct sign, if we compare the plot above the difference in the estimated step is 9 mm, 90% of the *true* step we added.
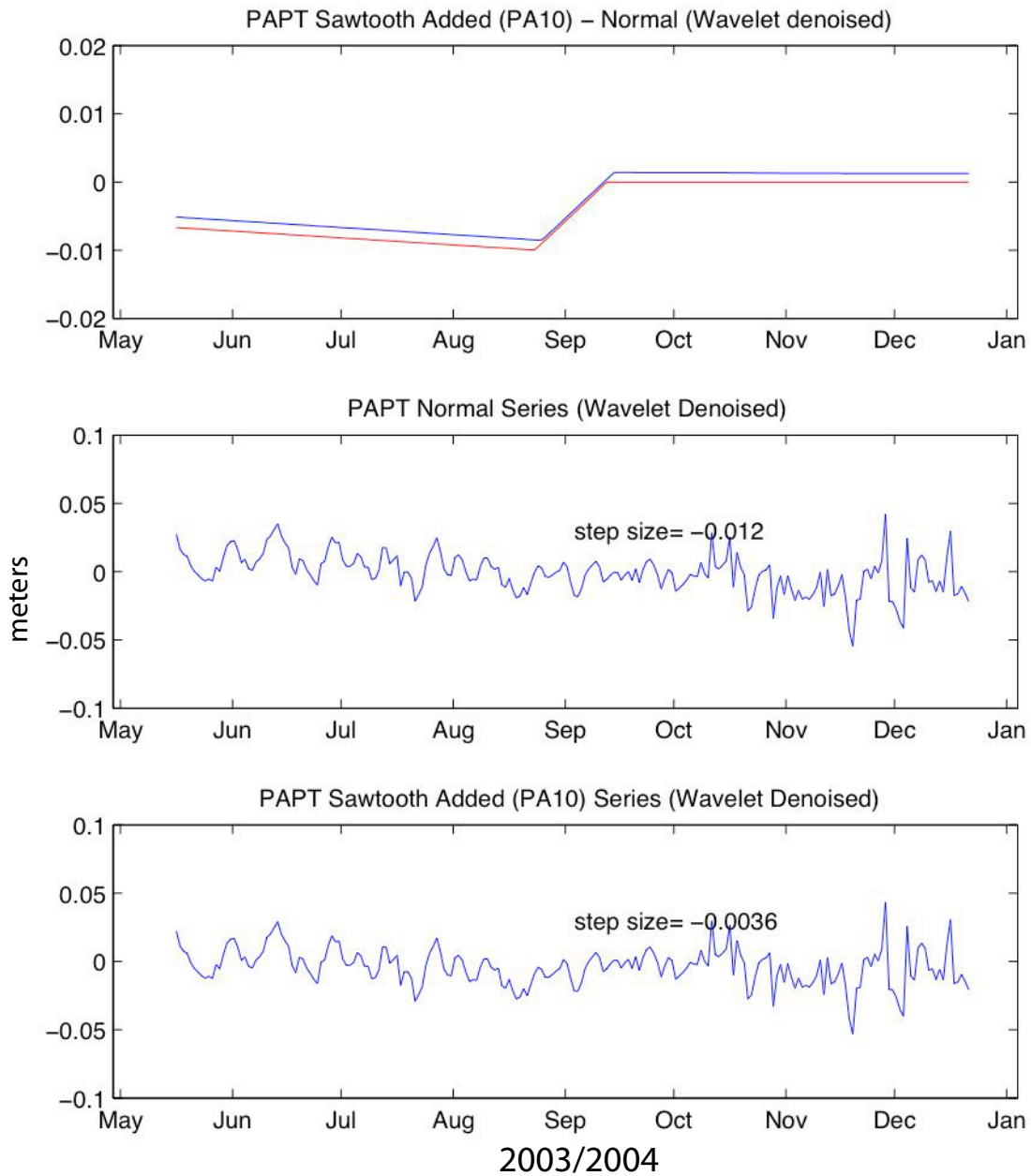
FIGURE 4.8. The result of adding a 10 mm step to the Port Angeles data set (the step is added to the same place as in the transfer function test). The denoising was done with the wavelet method. As in the the transfer function denoised window, there is a sizable negative step which happens to be there, unrelated to any tectonic process. In the bottom plot, which is the same window of data after denoising after an artificial step is added, we see that although the estimated step size (which should be 10 mm) does not even have the correct sign, if we compare the plot above, the difference in the estimated step is approximately 8 mm, 80% of the *true* step we added.

44

result that is consistent with that of the transfer function but with a difference in estimated step closer to 4 mm than 5 mm.

The advantage, then, from denoising is seen mostly after stacking events. If we look at the probability of finding a random step in any window, the benefit of denoising is demonstrated. For subtidal daily average relative water levels (not denoised) the standard deviation of the distribution of random steps is greater than that for transfer function denoised levels or wavelet denoised levels. This is especially true for pairs which are farther away from each other (Figure 4.10.). Comparing the sites in a pairwise fashion removes shared noise for closely located sites, but for distant sites which are more likely to have magnitude, phase, or character differences in noise response, denoising has a more pronounced effect than simple subtraction of one site from another without denoising.

Based on the above results of adding a artificial step, and comparison of errors, both for estimated water level changes during events and for a 12 event average, neither processing approach presents itself as clearly more efficacious. For individual events errors are greater than the estimated uplift in all but a few cases for both approaches[1], and in some of those few the estimated water level changes are not reasonable given GPS inversions of the location of slip along the fault interface and are likely due to actual water level changes (such anomalously large values often occur in pairs containing Seattle). So neither approach provides a satisfactory result for individual events.

Neither approach works near as well as we would like nor as well as we need to garner information on individual events. However, both processing approaches provide estimates for the average relative water level change during an event, which

---

[1]For detailed estimates of apparent water level changes after processing by both approaches see tables in Appendix A.
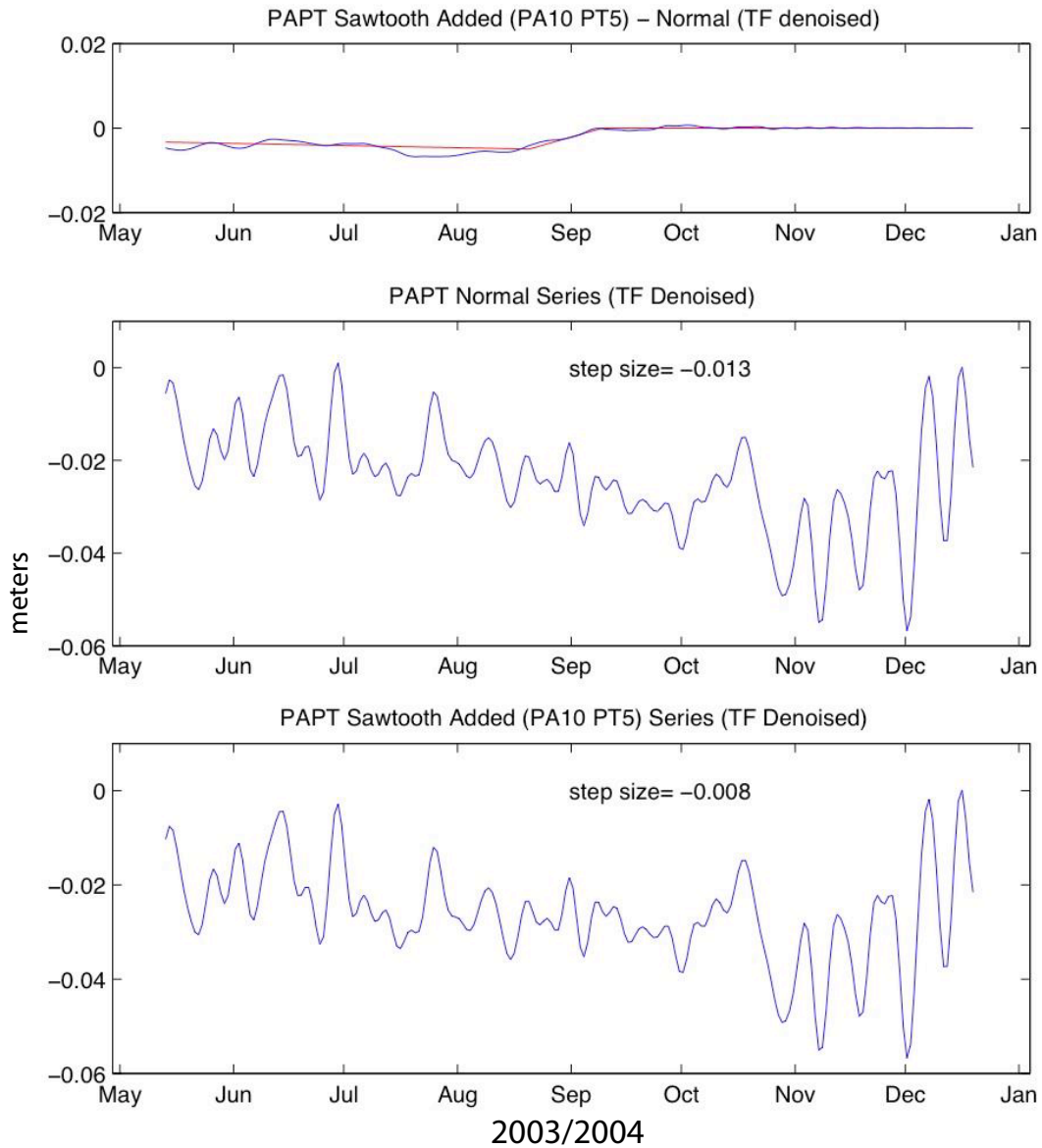
FIGURE 4.9. Artificial step test for steps added to both Port Angeles (10 mm) and Port Townsend (5 mm). See Figure 4.7. for more detailed explanation of the plots. As was the case when a step was added only to Port Angeles, The transfer function does not give an accurate estimate of the size of the step, however when comparing the original denoised data (middle) to the step from the data set with an artificial step, the difference is indeed 5 mm, as we expect to see.

46
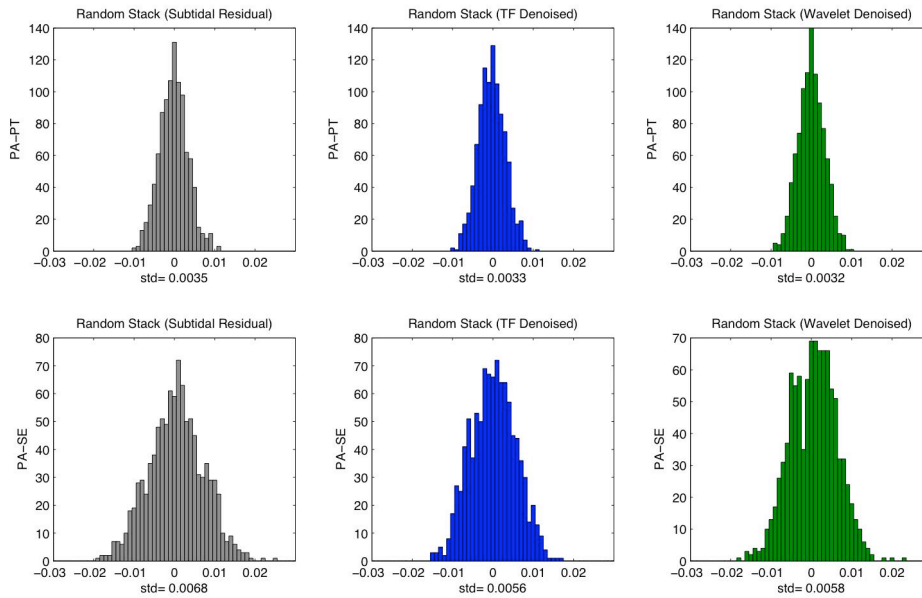
FIGURE 4.10. Distribution of step sized calculated from stacks of 12 randomly selected windows of data (Port Angeles relative to Port Townsend, top, and Port Angeles relative to Seattle, bottom). The grey (left) histogram in both is the distribution of step sizes from the subtidal residual (not denoised or filtered). The series denoised using the transfer function approach (blue) and the wavelet approach (green) have a narrower distribution of step sizes. For Port Angeles relative to Seattle (below) the improvement is larger. Further reduction in the probability of a step occurring that is not related to tectonic processes is achieved after removal of the residual relative seasonal cycle.

TABLE 4.1. Average apparent relative water level change for 12 ETS events (1997–2010) from Transfer function and Wavelet approaches and errors. Estimated water level changes for both processing methods are equal to each other and the predicted step (inferred from single site uplifts at individual stations from Table 2.1.) within the errors for all pairs except Neah Bay relative to Seattle.

Site pair	TF Step (mm)	Wav. Step (mm)	Pred. Step (mm)
PA-PT	-5.06 ± 1.36	-8.47 ± 3.38	-6.24 ± 1.76
PA-NB	-4.39 ± 2.43	-6.34 ± 3.96	-5.21 ± 1.98
PA-SE	-4.70 ± 3.15	-9.69 ± 5.64	-3.99 ± 2.20
NB-PT	0.93 ± 2.73	-1.85 ± 4.02	-1.03 ± 1.93
NB-SE	6.30 ± 3.49	-3.52 ± 5.72	1.22 ± 2.33
SE-PT	-7.56 ± 2.84	1.40 ± 6.38	-2.25 ± 2.16

are equal within their error bars (see Table 4.1.) for all pairs except Neah Bay relative to Seattle. These estimates, from both approaches, as well as single site estimates relative to a regional average from wavelet denoising, go into the least squares inversion to get an estimate of the average uplift at a single site.

CHAPTER V

CONCLUSION

Uplift during ETS in Cascadia is very small (millimeters) and it still lies on the very edge of the resolution of current technology. Although unable to overcome the tremendous noise in tide gauge records to reveal the uplift signal fro individual events, I have demonstrated that tide gauge records can be used to estimate average uplift during ETS. The average relative water level change for Port Angeles relative to Port Townsend is $-5.06\,\mathrm{mm}$ (from Table 4.1.).The distribution of step sizes from randomly chosen stack, we can see that such a large step falls on the very edges of that distribution. Thus it is very unlikely that this step is random. Instead we can conclude that it is the illusive uplift we sought all along, so we know the uplift for individual events is real and there for us to find if we can overcome the noise.

5.1. Limitations and Improvements

As mentioned in Chapter II, the proximity and similarity of tide gauges effects the efficacy of these processing methods. The Puget Sound is not a large enough body of water to be effected by a true tide. Rather, water level changes induced by the ocean tides propagate along its extent. In a similar way, far field ocean noise propagates throughout the Sound affecting each tide gauge as it passes. Many factors contribute to water level variations at a particular location as the amplitude and frequency content of the noise varies spatially. Both methods for removing noise rely on the forcing factors of the noise to be shared between sites, but how each point responds to the same forcing factor may be very different. For example wind from the open ocean blowing in an easterly direction along the Straight of Juan de Fuca

49

will tend to pile water up along one shore but not the other such that sites which are separated by only a few tens of kilometers can have very different water levels [*Pugh*, 2004].

Bathymetric and geographic differences will result in different amplitude responses to the same noise signal. Additionally, these same differences will produce different resonance phenomena. Increasing the number of sites that can be used for comparison would increase the likelihood of finding a pair which will have similar enough noise to facilitate efficacious denoising using either wavelet or transfer function approaches. Adding additional sites might also allow for greater resolution for individual events. By stacking multiple sites with similar uplift, noise might be reduced but the signal enhanced in much the same way it is when multiple events are stacked from one series (see Results section in Chapter II).

Denoising assumes only that two sites which are closely located will share noise, it does not take into account any of the actual causes of noise. Wind speed and direction, barometric pressure fluctuations, temperature induced expansion, increased inflow of water from land based sources, and meteorologically induced in or out fluxes of water all have an effect on water levels. The assumption that some of these factors are the same between locations, even those located as little as several tens of kilometers apart, may be incorrect. It is likely that some of the residual noise after denoising is due to factors with greater local heterogeneity. The seasonal differences might, for example, be caused, in part, by increased water volume from freshwater sources which are highly localized.

To attain resolutions high enough to reliably estimate single event uplift, it is possible that the general denoising approaches we have used thus far must be augmented with attempts to remove noise based on its particular source

(meteorological, from ocean basin oscillations, etc.) using further data: observations from weather stations, streamflow monitors, for example.

With further refinement of the methods presented here we may soon be able to resolve uplifts from individual events reliably. This would allow the use of this method for the study of ETS in locations around the world where GPS and seismic data are not available. Additionally tidal records could be used to study ETS in Cascadia before GPS data existed. There are tide gauge records in northern Washington going back nearly a century. Studying ETS in these records might tell us how the ETS cycle changes over the course of the megathrust cycle; how magnitude and recurrence interval change; how strain accumulation changes.

APPENDIX A

APPARENT WATER LEVEL CHANGE FROM TIDE GAUGE

RECORDS

TABLE A.1. Apparent relative water level changes due to ETS coseismic deformation (1997–2010) from transfer function denoised tide gauge records. Neah Bay, WA, Port Angeles, WA, Port Townsend, WA, and Seattle, WA were compared in a pairwise fashion and long term ocean oscillations were removed. Error bars for individual events are greater than the estimated water level change, except in the case of the largest events. Pairs which include Seattle or Neah bay consistently have the largest error. Neah Bay relative to Seattle has the largest error. For a detailed description of data processing, please see Chapter III, Data Analysis. Water level 'Step' is the difference of mean water level before and after an ETS event, a correction factor ('Corr') is applied to correct systematic bias (see Chapter IV, Error), the resultant corrected step ('corrStep') and total error ('totErr') are in bold. All values are in millimeters.

Year*	Site pair	Step	Err	randErr	Corr	corrErr	corrStep	totErr
1997	PA-PT	7.92	1.8	10.6	-2.49	0.24	**5.43**	**10.75**
	PA-NB	3.69	4.2	13.16	-2.35	0.48	**1.35**	**13.83**
	PA-SE	23.24	2.97	18.55	-0.79	0.44	**22.45**	**18.79**
	NB-PT	4.23	4.55	12.05	-0.1	0.5	**4.12**	**12.89**
	NB-SE	19.54	3.55	20.55	1.19	0.54	**20.73**	**20.86**
	SE-PT	-15.32	3.32	20.68	-1.46	0.46	**-16.77**	**20.95**
1998	PA-PT	-18.56	1.02	10.6	-2.49	0.24	**-21.05**	**10.65**
	PA-NB	-22.6	3.7	13.16	-2.35	0.48	**-24.95**	**13.68**
	PA-SE	1.79	3.5	18.55	-0.79	0.44	**1**	**18.88**
	NB-PT	4.04	3.73	12.05	-0.1	0.5	**3.94**	**12.62**
	NB-SE	24.39	4.22	20.55	1.19	0.54	**25.58**	**20.99**
	SE-PT	-20.34	3.42	20.68	-1.46	0.46	**-21.8**	**20.96**
1999	PA-PT	-16.52	1.37	10.6	-2.49	0.24	**-19.01**	**10.69**
	PA-NB	-20.13	2.72	13.16	-2.35	0.48	**-22.48**	**13.45**
	PA-SE	-19.91	2.66	18.55	-0.79	0.44	**-20.69**	**18.75**
	NB-PT	3.61	2.76	12.05	-0.1	0.5	**3.51**	**12.37**
	NB-SE	0.23	2.72	20.55	1.19	0.54	**1.42**	**20.74**
	SE-PT	3.39	2.56	20.68	-1.46	0.46	**1.93**	**20.84**
2000	PA-PT	-8.59	1.16	10.6	-2.49	0.24	**-11.08**	**10.67**
	PA-NB	3.5	2.72	13.16	-2.35	0.48	**1.16**	**13.45**
	PA-SE	36.53	3.15	18.55	-0.79	0.44	**35.74**	**18.82**
	NB-PT	-12.09	2.77	12.05	-0.1	0.5	**-12.2**	**12.37**
	NB-SE	33.02	3.87	20.55	1.19	0.54	**34.22**	**20.92**
	SE-PT	-45.12	3.29	20.68	-1.46	0.46	**-46.58**	**20.94**

* See Table C.1 for event start and end dates.

TABLE A.1. (continued)

Year[*]	Site pair	Step	Err	randErr	Corr	corrErr	corrStep	totErr
2002	PA-PT	-0.42	2.06	10.6	-2.49	0.24	**-2.91**	**10.8**
	PA-NB	11.41	2.65	13.16	-2.35	0.48	**9.06**	**13.44**
	PA-SE	-33.62	3.14	18.55	-0.79	0.44	**-34.41**	**18.82**
	NB-PT	-11.82	2.95	12.05	-0.1	0.5	**-11.93**	**12.41**
	NB-SE	-45.03	3.07	20.55	1.19	0.54	**-43.84**	**20.79**
	SE-PT	33.21	3.35	20.68	-1.46	0.46	**31.75**	**20.95**
2003	PA-PT	5.34	1.31	10.6	-2.49	0.24	**2.85**	**10.68**
	PA-NB	-0.28	3.03	13.16	-2.35	0.48	**-2.62**	**13.52**
	PA-SE	-26.98	2.75	18.55	-0.79	0.44	**-27.77**	**18.76**
	NB-PT	5.62	2.8	12.05	-0.1	0.5	**5.51**	**12.38**
	NB-SE	-26.7	2.93	20.55	1.19	0.54	**-25.51**	**20.77**
	SE-PT	32.32	2.39	20.68	-1.46	0.46	**30.86**	**20.82**
2004	PA-PT	-9.67	1.74	10.6	-2.49	0.24	**-12.16**	**10.75**
	PA-NB	-14.22	3.28	13.16	-2.35	0.48	**-16.57**	**13.57**
	PA-SE	-3.23	3.23	18.55	-0.79	0.44	**-4.01**	**18.83**
	NB-PT	4.55	3.67	12.05	-0.1	0.5	**4.45**	**12.6**
	NB-SE	10.99	3.48	20.55	1.19	0.54	**12.19**	**20.85**
	SE-PT	-6.44	3.5	20.68	-1.46	0.46	**-7.9**	**20.98**
2005	PA-PT	-26.03	1.57	10.6	-2.49	0.24	**-28.52**	**10.72**
	PA-NB	-15.18	3.2	13.16	-2.35	0.48	**-17.52**	**13.56**
	PA-SE	-35.08	2.78	18.55	-0.79	0.44	**-35.86**	**18.76**
	NB-PT	-10.85	3.18	12.05	-0.1	0.5	**-10.95**	**12.47**
	NB-SE	-19.9	3.84	20.55	1.19	0.54	**-18.71**	**20.92**
	SE-PT	9.05	3.29	20.68	-1.46	0.46	**7.59**	**20.94**
2007	PA-PT	2.25	1.79	10.6	-2.49	0.24	**-0.25**	**10.75**
	PA-NB	-9.02	3.98	13.16	-2.35	0.48	**-11.37**	**13.76**
	PA-SE	-13.1	3.47	18.55	-0.79	0.44	**-13.88**	**18.88**
	NB-PT	11.27	4.34	12.05	-0.1	0.5	**11.16**	**12.81**
	NB-SE	-4.08	4.84	20.55	1.19	0.54	**-2.89**	**21.12**
	SE-PT	15.35	3.6	20.68	-1.46	0.46	**13.89**	**20.99**
2008	PA-PT	-8.77	1.5	10.6	-2.49	0.24	**-11.26**	**10.71**
	PA-NB	6.19	3.28	13.16	-2.35	0.48	**3.85**	**13.58**
	PA-SE	18.65	2.25	18.55	-0.79	0.44	**17.87**	**18.69**
	NB-PT	-14.96	3.73	12.05	-0.1	0.5	**-15.07**	**12.62**
	NB-SE	12.46	4.24	20.55	1.19	0.54	**13.65**	**20.99**
	SE-PT	-27.42	2.32	20.68	-1.46	0.46	**-28.88**	**20.81**

[*] See Table C.1 for event start and end dates.

TABLE A.1. (continued)

Year*	Site pair	Step	Err	randErr	Corr	corrErr	corrStep	totErr
2009	PA-PT	1.19	1.97	10.6	-2.49	0.24	**-1.3**	**10.79**
	PA-NB	3.74	4.08	13.16	-2.35	0.48	**1.39**	**13.79**
	PA-SE	31.35	3.11	18.55	-0.79	0.44	**30.57**	**18.81**
	NB-PT	-2.55	3.71	12.05	-0.1	0.5	**-2.65**	**12.61**
	NB-SE	27.62	3.93	20.55	1.19	0.54	**28.81**	**20.93**
	SE-PT	-30.16	2.78	20.68	-1.46	0.46	**-31.62**	**20.87**
2010	PA-PT	-13.87	1.71	10.6	-2.49	0.24	**-16.36**	**10.74**
	PA-NB	-28.98	4.96	13.16	-2.35	0.48	**-31.33**	**14.07**
	PA-SE	-27.15	2.73	18.55	-0.79	0.44	**-27.94**	**18.75**
	NB-PT	11.88	4.97	12.05	-0.1	0.5	**11.77**	**13.04**
	NB-SE	-1.39	5	20.55	1.19	0.54	**-0.2**	**21.16**
	SE-PT	13.27	2.81	20.68	-1.46	0.46	**11.81**	**20.87**

* See Table C.1 for event start and end dates.

TABLE A.2. Average apparent relative water level change due ETS coseismic deformation (mean water level change for a stack of 12 events 1997-2010) from transfer function denoised tide gauge records. Neah Bay, WA, Port Angeles, WA, Port Townsend, WA, and Seattle, WA were compared in a pairwise fashion and long term ocean oscillations were removed. For a detailed description of data processing, please see Chapter III, Data Analysis. Water level 'Step' is the difference of mean water level before and after an ETS event, a correction factor ('Corr') is applied to correct systematic bias (see Chapter IV, Error), the resultant corrected step ('corrStep') and total error ('totErr') are in bold. All values are in millimeters.

Site pair	100day	100dErr	randErr	corr	corrErr	corrStep	totErr
PA-PT	-7.14	0.34	2.99	-2.49	0.24	**-9.64**	**3.02**
PA-NB	-6.82	0.91	3.71	-2.35	0.48	**-9.17**	**3.85**
PA-SE	-3.96	0.67	5.49	-0.79	0.44	**-4.74**	**5.55**
NB-PT	-0.59	0.96	3.51	-0.1	0.5	**-0.69**	**3.67**
NB-SE	2.6	0.93	6.02	1.19	0.54	**3.79**	**6.12**
SE-PT	-3.19	0.59	6.07	-1.46	0.46	**-4.64**	**6.11**

TABLE A.3.   Apparent relative water level changes due to ETS coseismic deformation (1997-2010) from wavelet transform denoised tide gauge records. Neah Bay, WA, Port Angeles, WA, Port Townsend, WA, and Seattle, WA were compared in a pairwise fashion and residual long term ocean oscillations were removed. Error bars for individual events are very large and greater than the estimated water level change, even in the case of the largest events. Pairs which include Seattle or Neah bay consistently have the largest error. For a detailed description of data processing, please see Chapter III, Data Analysis. Water level 'Step' is the difference of mean water level before and after an ETS event, a correction factor ('Corr') is applied to correct systematic bias (see Chapter IV, Error), the resultant corrected step ('corrStep') and total error ('totErr') are in bold. All values are in millimeters.

Year*	Site pair	Step	Err	randErr	Corr	corrErr	corrStep	totErr
1997	PA-PT	9.95	2.27	11.24	-2.20	0.29	**7.75**	**11.47**
	PA-NB	6.09	4.67	13.27	-2.53	0.52	**3.56**	**14.08**
	PA-SE	8.51	3.91	18.97	-2.38	0.52	**6.13**	**19.37**
	NB-PT	3.86	5.24	13.23	0.61	0.55	**4.47**	**14.24**
	NB-SE	2.42	5.21	18.41	-0.03	0.64	**2.40**	**19.14**
	SE-PT	1.44	3.89	22.24	0.36	0.50	**1.81**	**22.58**
1998	PA-PT	-23.47	1.47	11.24	-2.20	0.29	**-25.67**	**11.34**
	PA-NB	-22.53	4.03	13.27	-2.53	0.52	**-25.05**	**13.88**
	PA-SE	-18.32	3.82	18.97	-2.38	0.52	**-20.71**	**19.35**
	NB-PT	-0.94	3.96	13.23	0.61	0.55	**-0.33**	**13.82**
	NB-SE	4.20	3.34	18.41	-0.03	0.64	**4.17**	**18.72**
	SE-PT	-5.14	3.44	22.24	0.36	0.50	**-4.78**	**22.51**
1999	PA-PT	-14.34	2.22	11.24	-2.20	0.29	**-16.54**	**11.46**
	PA-NB	-15.74	3.47	13.27	-2.53	0.52	**-18.27**	**13.73**
	PA-SE	-19.22	3.85	18.97	-2.38	0.52	**-21.60**	**19.36**
	NB-PT	1.41	3.77	13.23	0.61	0.55	**2.01**	**13.76**
	NB-SE	-3.47	4.34	18.41	-0.03	0.64	**-3.50**	**18.92**
	SE-PT	4.88	3.35	22.24	0.36	0.50	**5.24**	**22.50**
2000	PA-PT	-5.67	1.82	11.24	-2.20	0.29	**-7.88**	**11.39**
	PA-NB	0.11	3.62	13.27	-2.53	0.52	**-2.42**	**13.76**
	PA-SE	40.00	3.86	18.97	-2.38	0.52	**37.62**	**19.36**
	NB-PT	-5.78	3.66	13.23	0.61	0.55	**-5.17**	**13.74**
	NB-SE	39.89	4.69	18.41	-0.03	0.64	**39.87**	**19.00**
	SE-PT	-45.68	3.74	22.24	0.36	0.50	**-45.31**	**22.56**

* See Table C.1 for event start and end dates.

TABLE A.3. (continued)

Year*	Site pair	Step	Err	randErr	Corr	corrErr	corrStep	totErr
2002	PA-PT	-0.04	2.76	11.24	-2.20	0.29	**-2.24**	**11.57**
	PA-NB	6.41	3.43	13.27	-2.53	0.52	**3.89**	**13.72**
	PA-SE	-17.00	4.06	18.97	-2.38	0.52	**-19.38**	**19.40**
	NB-PT	-6.45	3.97	13.23	0.61	0.55	**-5.84**	**13.82**
	NB-SE	-23.41	4.62	18.41	-0.03	0.64	**-23.44**	**18.99**
	SE-PT	16.96	3.70	22.24	0.36	0.50	**17.33**	**22.55**
2003	PA-PT	11.32	2.30	11.24	-2.20	0.29	**9.12**	**11.47**
	PA-NB	4.23	4.07	13.27	-2.53	0.52	**1.70**	**13.89**
	PA-SE	-23.47	4.07	18.97	-2.38	0.52	**-25.86**	**19.40**
	NB-PT	7.10	3.93	13.23	0.61	0.55	**7.71**	**13.81**
	NB-SE	-27.70	4.32	18.41	-0.03	0.64	**-27.73**	**18.92**
	SE-PT	34.80	3.03	22.24	0.36	0.50	**35.16**	**22.45**
2004	PA-PT	-12.42	1.55	11.24	-2.20	0.29	**-14.62**	**11.35**
	PA-NB	-10.56	3.44	13.27	-2.53	0.52	**-13.09**	**13.72**
	PA-SE	-10.09	2.96	18.97	-2.38	0.52	**-12.48**	**19.20**
	NB-PT	-1.86	3.85	13.23	0.61	0.55	**-1.25**	**13.79**
	NB-SE	0.46	3.97	18.41	-0.03	0.64	**0.44**	**18.84**
	SE-PT	-2.32	2.81	22.24	0.36	0.50	**-1.96**	**22.42**
2005	PA-PT	-28.17	1.93	11.24	-2.20	0.29	**-30.38**	**11.40**
	PA-NB	-19.31	3.81	13.27	-2.53	0.52	**-21.84**	**13.82**
	PA-SE	-40.80	3.40	18.97	-2.38	0.52	**-43.19**	**19.27**
	NB-PT	-8.86	4.19	13.23	0.61	0.55	**-8.25**	**13.89**
	NB-SE	-21.49	4.48	18.41	-0.03	0.64	**-21.52**	**18.96**
	SE-PT	12.63	3.38	22.24	0.36	0.50	**12.99**	**22.50**
2007	PA-PT	4.81	2.56	11.24	-2.20	0.29	**2.61**	**11.53**
	PA-NB	-10.36	3.76	13.27	-2.53	0.52	**-12.89**	**13.80**
	PA-SE	-11.34	4.98	18.97	-2.38	0.52	**-13.72**	**19.62**
	NB-PT	15.17	4.37	13.23	0.61	0.55	**15.78**	**13.94**
	NB-SE	-0.98	5.98	18.41	-0.03	0.64	**-1.00**	**19.36**
	SE-PT	16.15	4.58	22.24	0.36	0.50	**16.51**	**22.71**
2008	PA-PT	-7.23	2.27	11.24	-2.20	0.29	**-9.43**	**11.47**
	PA-NB	12.48	3.43	13.27	-2.53	0.52	**9.95**	**13.72**
	PA-SE	9.05	2.79	18.97	-2.38	0.52	**6.66**	**19.18**
	NB-PT	-19.71	4.32	13.23	0.61	0.55	**-19.10**	**13.93**
	NB-SE	-3.43	4.29	18.41	-0.03	0.64	**-3.46**	**18.91**
	SE-PT	-16.28	2.86	22.24	0.36	0.50	**-15.91**	**22.43**

* See Table C.1 for event start and end dates.

Year*	Site pair	Step	Err	randErr	Corr	corrErr	corrStep	totErr
2009	PA-PT	1.94	2.05	11.24	-2.20	0.29	**-0.26**	**11.43**
	PA-NB	4.65	3.60	13.27	-2.53	0.52	**2.12**	**13.76**
	PA-SE	19.54	3.14	18.97	-2.38	0.52	**17.16**	**19.23**
	NB-PT	-2.71	3.70	13.23	0.61	0.55	**-2.10**	**13.75**
	NB-SE	14.90	4.12	18.41	-0.03	0.64	**14.87**	**18.87**
	SE-PT	-17.60	2.61	22.24	0.36	0.50	**-17.24**	**22.40**
2010	PA-PT	-11.86	4.00	11.24	-2.20	0.29	**-14.06**	**11.93**
	PA-NB	-1.16	5.76	13.27	-2.53	0.52	**-3.69**	**14.47**
	PA-SE	-24.47	5.19	18.97	-2.38	0.52	**-26.86**	**19.67**
	NB-PT	-10.69	4.30	13.23	0.61	0.55	**-10.08**	**13.92**
	NB-SE	-23.31	4.79	18.41	-0.03	0.64	**-23.33**	**19.03**
	SE-PT	12.61	3.54	22.24	0.36	0.50	**12.98**	**22.52**

* See Table C.1 for event start and end dates.

TABLE A.4. Average apparent relative water level change due ETS coseismic deformation (mean water level change for a stack of 12 events 1997-2010) from wavelet decomposition denoised tide gauge records. Neah Bay, WA, Port Angeles, WA, Port Townsend, WA, and Seattle, WA were compared in a pairwise fashion and residual long term ocean oscillations were removed. For a detailed description of data processing, please see Chapter III, Data Analysis. Water level 'Step' is the difference of mean water level before and after an ETS event, a correction factor ('Corr') is applied to correct systematic bias (see Chapter IV, Error), the resultant corrected step ('corrStep') and total error ('totErr') are in bold. All values are in millimeters.

Site pair	100day	100dErr	randErr	corr	corrErr	corrStep	totErr
PA-PT	-6.26	0.63	3.31	-2.20	0.29	**-8.47**	**3.38**
PA-NB	-3.81	1.02	3.79	-2.53	0.52	**-6.34**	**3.96**
PA-SE	-7.30	1.02	5.53	-2.38	0.52	**-9.69**	**5.64**
NB-PT	-2.46	1.10	3.83	0.61	0.55	**-1.85**	**4.02**
NB-SE	-3.49	1.27	5.54	-0.03	0.64	**-3.52**	**5.72**
SE-PT	1.04	0.74	6.32	0.36	0.50	**1.40**	**6.38**

TABLE A.5.   Apparent water level changes due to ETS coseismic deformation(1997-2010) from wavelet transform denoised tide gauge records at Neah Bay, WA, Port Angeles, WA, Port Townsend, WA, and Seattle, WA (water level changes are relative to a regional average). Residual long term ocean oscillations were removed. Error bars for individual events are very large and greater than the estimated water level change, even in the case of the largest events. For a detailed description of data processing, please see Chapter III, Data Analysis. Water level 'Step' is the difference of mean water level before and after an ETS event, a correction factor ('Corr') is applied to correct systematic bias (see Chapter IV, Error), the resultant corrected step ('corrStep') and total error ('totErr') are in bold. All values are in millimeters.

Year*	Site	Step	Err	randErr	Corr	corrErr	corrStep	totErr
1997	PA	7.05	2.46	11.37	-2.24	0.33	**4.81**	**11.63**
	PT	-1.27	2.49	10.70	0.13	0.28	**-1.15**	**10.99**
	NB	3.43	3.43	9.19	-0.02	0.39	**3.41**	**9.82**
	SE	-2.25	2.38	12.13	-0.15	0.31	**-2.39**	**12.37**
1998	PA	-21.27	2.55	11.37	-2.24	0.33	**-23.51**	**11.66**
	PT	2.67	2.17	10.70	0.13	0.28	**2.80**	**10.93**
	NB	0.26	2.26	9.19	-0.02	0.39	**0.23**	**9.48**
	SE	-3.16	1.78	12.13	-0.15	0.31	**-3.30**	**12.27**
1999	PA	-16.49	2.36	11.37	-2.24	0.33	**-18.73**	**11.61**
	PT	-3.82	1.85	10.70	0.13	0.28	**-3.69**	**10.87**
	NB	-0.18	2.59	9.19	-0.02	0.39	**-0.20**	**9.56**
	SE	2.95	2.19	12.13	-0.15	0.31	**2.81**	**12.33**
2000	PA	13.82	2.21	11.37	-2.24	0.33	**11.58**	**11.59**
	PT	20.50	1.89	10.70	0.13	0.28	**20.63**	**10.87**
	NB	12.57	2.68	9.19	-0.02	0.39	**12.55**	**9.59**
	SE	-28.35	2.42	12.13	-0.15	0.31	**-28.49**	**12.38**
2002	PA	-6.41	2.47	11.37	-2.24	0.33	**-8.65**	**11.64**
	PT	-5.72	2.01	10.70	0.13	0.28	**-5.59**	**10.90**
	NB	-11.38	2.71	9.19	-0.02	0.39	**-11.40**	**9.59**
	SE	14.56	2.39	12.13	-0.15	0.31	**14.41**	**12.37**
2003	PA	-3.21	2.81	11.37	-2.24	0.33	**-5.45**	**11.72**
	PT	-15.94	1.79	10.70	0.13	0.28	**-15.81**	**10.86**
	NB	-7.50	2.69	9.19	-0.02	0.39	**-7.52**	**9.59**
	SE	20.04	2.03	12.13	-0.15	0.31	**19.89**	**12.30**

* See Table C.1 for event start and end dates.

TABLE A.5. (continued)

Year*	Site	Step	Err	randErr	Corr	corrErr	corrStep	totErr
2004	PA	-9.36	1.80	11.37	-2.24	0.33	**-11.60**	**11.51**
	PT	2.52	1.74	10.70	0.13	0.28	**2.65**	**10.85**
	NB	1.02	2.59	9.19	-0.02	0.39	**1.00**	**9.56**
	SE	-2.82	1.78	12.13	-0.15	0.31	**-2.97**	**12.27**
2005	PA	-30.03	2.08	11.37	-2.24	0.33	**-32.27**	**11.56**
	PT	-1.02	2.00	10.70	0.13	0.28	**-0.89**	**10.89**
	NB	-12.94	2.85	9.19	-0.02	0.39	**-12.96**	**9.63**
	SE	12.41	2.11	12.13	-0.15	0.31	**12.26**	**12.32**
2007	PA	-6.40	2.61	11.37	-2.24	0.33	**-8.64**	**11.67**
	PT	-12.28	2.24	10.70	0.13	0.28	**-12.16**	**10.94**
	NB	6.15	3.32	9.19	-0.02	0.39	**6.13**	**9.78**
	SE	4.96	3.09	12.13	-0.15	0.31	**4.82**	**12.53**
2008	PA	0.14	1.78	11.37	-2.24	0.33	**-2.10**	**11.51**
	PT	11.56	1.91	10.70	0.13	0.28	**11.69**	**10.88**
	NB	-9.60	2.86	9.19	-0.02	0.39	**-9.62**	**9.63**
	SE	-5.13	1.85	12.13	-0.15	0.31	**-5.28**	**12.28**
2009	PA	12.92	2.19	11.37	-2.24	0.33	**10.68**	**11.58**
	PT	7.38	1.55	10.70	0.13	0.28	**7.51**	**10.82**
	NB	5.32	2.63	9.19	-0.02	0.39	**5.30**	**9.57**
	SE	-10.72	1.83	12.13	-0.15	0.31	**-10.86**	**12.27**
2010	PA	-16.48	4.36	11.37	-2.24	0.33	**-18.72**	**12.18**
	PT	-4.80	2.05	10.70	0.13	0.28	**-4.67**	**10.90**
	NB	-1.54	2.97	9.19	-0.02	0.39	**-1.56**	**9.67**
	SE	13.60	2.28	12.13	-0.15	0.31	**13.45**	**12.35**

* See Table C.1 for event start and end dates.

TABLE A.6. Average apparent water level change due ETS coseismic deformation (mean water level change for a stack of 12 events 1997-2010) from wavelet decomposition denoised tide gauge records at Neah Bay, WA, Port Angeles, WA, Port Townsend, WA, and Seattle, WA (water level changes are relative to a regional average). Residual long term ocean oscillations were removed. For a detailed description of data processing, please see Chapter III, Data Analysis. Water level 'Step' is the difference of mean water level before and after an ETS event, a correction factor ('Corr') is applied to correct systematic bias (see Chapter IV, Error), the resultant corrected step ('corrStep') and total error ('totErr') are in bold. All values are in millimeters.

Site	100day	100dErr	randErr	corr	corrErr	corrStep	totErr
PA	-6.31	0.67	3.32	-2.24	0.33	**-8.55**	**3.40**
PT	-0.02	0.44	2.83	0.13	0.28	**0.11**	**2.88**
NB	-1.20	0.79	2.54	-0.02	0.39	**-1.22**	**2.69**
SE	1.34	0.56	3.72	-0.15	0.31	**1.20**	**3.77**

APPENDIX B

ESTIMATED COSEISMIC UPLIFT DURING ETS

(1997-2010)

TABLE B.1. Per event coseismic uplift during ETS from a least squares inversion of apparent relative water level changes at Neah Bay, WA, Port Angeles, WA, Port Townsend, WA, and Seattle, WA. All values are in millimeters.

Year*	Site			Uplift
1997	NB	−1.65	±	1.51
	PA	−1.73	±	1.24
	PT	0.30	±	1.25
	SE	3.08	±	1.77
1998	NB	−7.89	±	2.90
	PA	7.69	±	2.38
	PT	−6.58	±	2.42
	SE	6.78	±	3.45
1999	NB	−1.55	±	2.55
	PA	6.26	±	2.12
	PT	−3.56	±	2.16
	SE	−1.15	±	3.08
2000	NB	−5.01	±	2.72
	PA	−3.56	±	2.25
	PT	−9.18	±	2.29
	SE	17.75	±	3.28
2002	NB	6.61	±	1.26
	PA	4.84	±	1.06
	PT	0.20	±	1.08
	SE	−11.65	±	1.52
2003	NB	−0.64	±	3.12
	PA	2.46	±	2.59
	PT	4.63	±	2.62
	SE	−6.46	±	3.75
2004	NB	−4.36	±	1.25
	PA	5.06	±	1.03
	PT	−0.75	±	1.06
	SE	0.06	±	1.49

* See Table C.1 for event start and end dates.

TABLE B.1. (continued)

Year*	Site			Uplift
2005	NB	3.68	±	3.22
	PA	10.54	±	2.66
	PT	−3.39	±	2.71
	SE	−10.82	±	3.84
2007	NB	−7.43	±	1.56
	PA	4.49	±	1.28
	PT	4.16	±	1.30
	SE	−1.22	±	1.84
2008	NB	4.72	±	1.73
	PA	0.15	±	1.42
	PT	−10.21	±	1.45
	SE	5.35	±	2.05
2009	NB	−3.50	±	1.09
	PA	−3.71	±	0.91
	PT	−5.59	±	0.92
	SE	12.81	±	1.29
2010	NB	−0.21	±	2.39
	PA	7.75	±	1.95
	PT	2.16	±	1.96
	SE	−9.70	±	2.76

* See Table C.1 for event start and end dates.

APPENDIX C

ETS EVENT DATES

TABLE C.1. ETS dates for processing. The middle day of the event (Event Mid. Day) is calculated from GPS derived start and end dates for deformation at Port Angeles. Event start and end days (Event Start/End) are the first and twentieth day of a twenty day window centered on the middle day. 100 day window start and end days (100dy. Start/End),are one hundred days before and after the event start and end days.

Year	100dy St.	Event St.	Event Mid	Event End	100dy End
1997	15-Jan-1997	25-Apr-1997	5-May-1997	14-May-1997	22-Aug-1997
1998	21-Mar-1998	29-Jun-1998	9-Jul-1998	18-Jul-1998	26-Oct-1998
1999	14-May-1999	22-Aug-1999	1-Sep-1999	10-Sep-1999	19-Dec-1999
2000	19-Aug-2000	27-Nov-2000	7-Dec-2000	16-Dec-2000	26-Mar-2001
2002	17-Oct-2001	25-Jan-2002	4-Feb-2002	13-Feb-2002	24-May-2002
2003	13-Nov-2002	21-Feb-2003	3-Mar-2003	12-Mar-2003	20-Jun-2003
2004	27-Mar-2004	5-Jul-2004	15-Jul-2004	24-Jul-2004	1-Nov-2004
2005	25-May-2005	2-Sep-2005	12-Sep-2005	21-Sep-2005	30-Dec-2005
2007	13-Oct-2006	21-Jan-2007	31-Jan-2007	9-Feb-2007	20-May-2007
2008	27-Jan-2008	6-May-2008	16-May-2008	25-May-2008	2-Sep-2008
2009	25-Jan-2009	5-May-2009	15-May-2009	24-May-2009	1-Sep-2009
2010	27-Apr-2010	5-Aug-2010	15-Aug-2010	24-Aug-2010	2-Dec-2010

[*] See Table C.1 for event start and end dates.

LEAST SQUARES INVERSION OF WATER LEVELS

D.1. Uplift During ETS

Given the observational constraints of relative water level changes for each ETS event, I preform an inversion to find the site specific uplift. For single site apparent water level change estimates we could simply multiply by -1 to get an estimate of vertical uplift, however, as mentioned previously the uncertainties on single site estimates are very large. Let:

$$-NB = u = \text{uplift at Neah Bay}$$

$$-PA = w = \text{uplift at Port Angeles}$$

$$-PT = y = \text{uplift at Port Townsend}$$

$$-SE = z = \text{uplift at Seattle}$$

Relative apparent water level changes generally have smaller uncertainties. However, multiplying by -1, only results in *relative* uplift during an ETS event. To take advantage of the benefits of comparing sites in a pairwise fashion in the estimation of *single* site uplifts we utilize a least squares adjustment. We compare all four sites in a pairwise fashion in such a way that, on average, we would expect to see a negative relative water level step, for the sake of consistency[1] Relative water level change

---

[1]We order them according to GPS average per event uplift, for example, in general, Port Angeles goes up during ETS (the water level should drop) and Neah Bay also goes up (the water goes down), though not as much, so we would subtract Neah Bay from Port Angeles (negative water level− less negative water level= negative *relative* water level)

observations after denoising are constraints for the Least Squares Inversion:

$$w - y = C_1 \pm v_1 \quad C_1 = \text{Constraint 1(from measured PA-PT)} \quad \text{(Equation D.1.a)}$$

$$w - u = C_2 \pm v_2 \quad C_2 = \text{Constraint 2 (from measured PA-NB)} \quad \text{(Equation D.1.b)}$$

$$w - z = C_3 \pm v_3 \quad C_3 = \text{Constraint 3 (from measured PA-SE)} \quad \text{(Equation D.1.c)}$$

$$u - y = C_4 \pm v_4 \quad C_4 = \text{Constraint 4 (from measured NB-PT)} \quad \text{(Equation D.1.d)}$$

$$u - z = C_5 \pm v_5 \quad C_5 = \text{Constraint 5 (from measured NB-SE)} \quad \text{(Equation D.1.e)}$$

$$z - y = C_6 \pm v_6 \quad C_6 = \text{Constraint 6 (from measured SE-PT)} \quad \text{(Equation D.1.f)}$$

where v_i is the "redidual", or computed minus the measured value. We can also add single site uplifts relative to a regional average (from wavelet denoising).

$$\text{average} - NB = \quad u - \left(\frac{u + w + y + z}{4} \right) = C_7 \pm v_7$$

$$= \quad \frac{3u - w - y - z}{4} = C_7 \pm v_7 \quad \text{(Equation D.2.a)}$$

Similarly:

$$\text{average} - PA = \quad \frac{3w - u - y - z}{4} = C_8 \pm v_8 \quad \text{(Equation D.2.b)}$$

$$\text{average} - PT = \quad \frac{3y - u - w - z}{4} = C_9 \pm v_9 \quad \text{(Equation D.2.c)}$$

$$\text{average} - SE = \quad \frac{3z - u - w - y}{4} = C_{10} \pm v_{10} \quad \text{(Equation D.2.d)}$$

In matrix form, the constraints[2] are $\mathbf{L} = C_i$, and corresponding residuals are $\mathbf{V} = v_i$. The matrix, $\mathbf{U}$, for the computed uplifts at a single site and the normal coefficient matrix, $\mathbf{A}$, are:

$$\mathbf{A} = \begin{pmatrix} 0 & 1 & -1 & 0 \\ -1 & 1 & 0 & 0 \\ 0 & 1 & 0 & -1 \\ 1 & 0 & -1 & 0 \\ 1 & 0 & 0 & -1 \\ 0 & 0 & -1 & 1 \\ 0 & 1 & -1 & 0 \\ -1 & 1 & 0 & 0 \\ 0 & 1 & 0 & -1 \\ 1 & 0 & -1 & 0 \\ 1 & 0 & 0 & -1 \\ 0 & 0 & -1 & 1 \\ \frac{3}{4} & \frac{1}{4} & \frac{1}{4} & \frac{1}{4} \\ \frac{1}{4} & \frac{3}{4} & \frac{1}{4} & \frac{1}{4} \\ \frac{1}{4} & \frac{1}{4} & \frac{3}{4} & \frac{1}{4} \\ \frac{1}{4} & \frac{1}{4} & \frac{1}{4} & \frac{3}{4} \end{pmatrix} \qquad \mathbf{U} = \begin{pmatrix} u \\ w \\ y \\ z \end{pmatrix}$$

We know from Equations Equation D.1. and Equation D.2. that

$$\mathbf{AU} = \mathbf{L} + \mathbf{V} \qquad \qquad \text{(Equation D.3.)}$$

---

[2]including relative uplifts from both transfer function denoised and wavelet denoised data, as well as single site uplifts relative to the regional average

To get the most probable values for single site uplift during ETS based on relative water level changes we can solve for $\mathbf{U}$ using [*Wolf and Ghilani*, 2002]:

$$\mathbf{U} = \left(\mathbf{A}^T\mathbf{A}\right)^{-1}\mathbf{A}^T\mathbf{L} \qquad \text{(Equation D.4.)}$$

To do a weighted least squares adjustment we must add a weight matrix, $\mathbf{W}$, which is a diagonal square matrix with size equal to the length of $\mathbf{L}$. The weights are uncertainties, σ_t^{-2}, from water level change estimation, see Chapter II, Methods, and Chapter IV for a detailed explanation. For a *weighted* least squares estimate of the most probable value for uplift at our four sites we use the weighted version of Equation Equation D.4. [*Wolf and Ghilani*, 2002]:

$$\mathbf{U} = \left(\mathbf{A}^T\mathbf{W}\mathbf{A}\right)^{-1}\mathbf{A}^T\mathbf{W}\mathbf{L} \qquad \text{(Equation D.5.)}$$

The residuals (calculated-observed), v_i, can be calculated with:

$$\mathbf{V} = \mathbf{A}\mathbf{U} - \mathbf{L} \qquad \text{(Equation D.6.)}$$

And the standard deviation of unit weight is:

$$\sigma_0 = \sqrt{\frac{\mathbf{V}^T\mathbf{W}\mathbf{V}}{n}} \qquad \text{(Equation D.7.)}$$

where n =degrees of freedom, which is observations (constraints) minus unknowns, which in this case is $16 - 4 = 12$. The estimated standard deviation in adjusted uplift estimates for our four sites is given by, $\sigma_{u_i} = \sigma_0\sqrt{q_{u_i u_i}}$, where $q_{u_i u_i}$ is the diagonal of

$$\mathbf{Q} = \left(\mathbf{A}^T\mathbf{W}\mathbf{A}\right)^{-1} \quad \text{covariance matrix} \qquad \text{(Equation D.8.)}$$

D.2. ETS Interseismic Uplift

We use the above technique to calculate interseismic uplift between events. Our unknowns, x_i, are annual uplift rates at our four NOAA stations. Our constraints this time are annual relative uplift rates of change for all six pairs from transfer function denoised data. In addition we add long term annual uplift rates, r_i, at the four sites estimated using long term leveling and tide gauge record estimates from the work of *Burgette et al.* [2009] and the adjusted single site estimates from above. An average *annual* uplift rate from ETS seismic is calculated and subtracted from long term uplift to ETS interseismic uplift, so, $x_i = ri - u_i$.

$$
\mathbf{A} =
\begin{pmatrix}
0 & 1 & -1 & 0 \\
-1 & 1 & 0 & 0 \\
0 & 1 & 0 & -1 \\
1 & 0 & -1 & 0 \\
1 & 0 & 0 & -1 \\
0 & 0 & -1 & 1 \\
0 & 1 & 0 & 0 \\
0 & 0 & 1 & 0 \\
1 & 0 & 0 & 0 \\
0 & 0 & 0 & 1
\end{pmatrix}
$$

The weight matrix, $\mathbf{W}$, again has diagonal elements which are the inverse square of the total error, σ_t^{-2}, for each observation. For the last four constraints the uncertainties from the least squares adjustement, σ_{u_i}, and the uncertainties on the long term uplifts, from *Verdonck* [2006] (see Table 2.1. for values, are added in quadrature. The

procedure outlined in the first section of this appendix is followed to get adjusted interseismic uplifts rates at all 4 sites with uncertainties (see Table 2.1.).

REFERENCES CITED

Burgette, R., R. Weldon, and D. Schmidt, Interseismic uplift rates for western oregon and along-strike variation in locking on the cascadia subduction zone, *J. Geophys. Res.*, *114*, B01,408, 2009.

Chapman, J., and T. Melbourne, Future cascadia megathrust rupture delineated by episodic tremor and slip, *Geophys. Res. Lett*, *36*(22), L22,301, 2009.

Dragert, H., K. Wang, and T. James, A silent slip event on the deeper cascadia subduction interface, *Science*, *292*(5521), 1525, 2001.

Gomberg, J., and et al., Slow slip phenomena in cascadia from 2007 and beyond: A review., *GSA Bull.*, *122*, 963 – 978, 2010.

Goring, D., Extracting long waves from tide-gauge records, *J. Waterw. Port Coast. Ocean Eng.*, *134*, 306, 2008.

Hirose, H., K. Hirahara, F. Kimata, N. Fujii, and S. Miyazaki, A slow thrust slip event following the two 1996 hyuganada earthquakes beneath the bungo channel, southwest japan, *Geophys. Res. Lett*, *26*(21), 3237–3240, 1999.

Jacoby, G., D. Bunker, and B. Benson, Tree-ring evidence for an ad 1700 cascadia earthquake in washington and northern oregon, *Geology*, *25*(11), 999, 1997.

Krauss, T., L. Shure, and J. Little, *Signal Processing Toolbox for Use with MATLAB®: User's Guide*, The MathWorks Inc., Natick, Massachusetts, 1994.

Matsuzawa, T., H. Hirose, B. Shibazaki, and K. Obara, Modeling short-and long-term slow slip events in the seismic cycles of large subduction earthquakes, *J. Geophys. Res.*, *115*(B12), B12,301, 2010.

McCaffrey, R., A. Qamar, R. King, R. Wells, G. Khazaradze, C. Williams, C. Stevens, J. Vollick, and P. Zwick, Fault locking, block rotation and crustal deformation in the pacific northwest, *Geophys. J. Int.*, *169*(3), 1315–1340, 2007.

McGuire, J., and P. Segall, Imaging of aseismic fault slip transients recorded by dense geodetic networks, *Geophys. J. Int.*, *155*(3), 778–788, 2003.

Melbourne, T., W. Szeliga, M. Miller, and V. Santillan, Extent and duration of the 2003 cascadia slow earthquake, *Geophys. Res. Lett*, *32*, 1997–2005, 2005.

Miller, M., T. Melbourne, D. Johnson, and W. Sumner, Periodic slow earthquakes from the cascadia subduction zone, *Science*, *295*(5564), 2423, 2002.

Misiti, M., Y. Misiti, G. Oppenheim, and J. Poggi, *Wavelet Toolbox^{TM} 4: Mathlab User's Guide*, The MathWorks Inc., Natick, Massachusetts, 1997.

Nelson, A., et al., Radiocarbon evidence for extensive plate-boundary rupture about 300 years ago at the cascadia subduction zone, *Nature*, *378*, 371–374, 1995.

Obara, K., Nonvolcanic deep tremor associated with subduction in southwest japan, *Science*, *296*(5573), 1679, 2002.

Obara, K., H. Hirose, F. Yamamizu, and K. Kasahara, Episodic slow slip events accompanied by non-volcanic tremors in southwest japan subduction zone, *Geophys. Res. Lett*, *31*(4), 2004.

Payero, J., V. Kostoglodov, N. Shapiro, T. Mikumo, A. Iglesias, X. Pérez-Campos, and R. Clayton, Nonvolcanic tremor observed in the mexican subduction zone, *Geophys. Res. Lett*, *35*(7), Art–No, 2008.

Pugh, D., *Changing Sea Levels: Effects of Tides, Weather, and Climate*, Cambridge Univ. Press, Cambridge, UK, 2004.

Reid, H., A. Lawson, and S. E. I. Commission, *The California Earthquake of April 18, 1906*, Carnegie Institute of Washington, Washington D.C.

Rogers, G., and H. Dragert, Episodic tremor and slip on the cascadia subduction zone: The chatter of silent slip, *Science*, *300*(5627), 1942, 2003.

Satake, K., K. Shimazaki, Y. Tsuji, and K. Ueda, Time and size of a giant earthquake in cascadia inferred from japanese tsunami records of january 1700, *Nature*, *379*(6562), 246–249, 1996.

Savage, J., M. Lisowski, and W. Prescott, Strain accumulation in western washington, *J. Geophys. Res.*, *96*(B9), 14,493–14, 1991.

Schmidt, D., and H. Gao, Source parameters and time-dependent slip distributions of slow slip events on the cascadia subduction zone from 1998 to 2008, *J. Geophys. Res.*, *115*, 2010.

Schwartz, S. Y., and J. M. Rokosky, Slow slip events and seismic tremor at circum-pacific subduction zones, *Rev. Geophys.*, *45*, 2007.

Shelly, D., G. Beroza, S. Ide, and S. Nakamula, Low-frequency earthquakes in shikoku, japan, and their relationship to episodic tremor and slip, *Nature*, *442*(7099), 188–191, 2006.

Szeliga, W., T. Melbourne, M. Miller, and V. Santillan, Southern cascadia episodic slow earthquakes, *Geophys. Res. Lett*, *31*, L16,602, 2004.

Szeliga, W., T. Melbourne, M. Santillan, and M. Miller, Gps constraints on 34 slow slip events within the cascadia subduction zone, 1997–2005, *J. Geophys. Res.*, *113*(B4), B04,404, 2008.

Verdonck, D., Contemporary vertical crustal deformation in cascadia, *Tectonophysics*, *417*(3-4), 221–230, 2006.

Wang, K., R. Wells, S. Mazzotti, R. Hyndman, and T. Sagiya, A revised dislocation model of interseismic deformation of the cascadia subduction zone, *J. Geophys. Res.*, *108*(10.1029), 2003.

Wech, A., K. Creager, and T. Melbourne, Seismic and geodetic constraints on cascadia slow slip, *J. Geophys. Res.*, *114*(B10), B10,316, 2009.

Wei, W., *Time Series Analysis*, Addison-Wesley, Redwood City, California, 1994.

Wells, R., and R. Simpson, Northward migration of the cascadia forearc in the northwestern us and implications for subduction deformation, *Earth Planets and Space*, *53*(4), 275–284, 2001.

Wolf, P., and C. Ghilani, *Elementary Surveying: An Introduction to Geomatics*, Prentice Hall, Upper Saddle River, New Jersey, 2002.

Yamaguchi, D., B. Atwater, D. Bunker, B. Benson, and M. Reid, Tree-ring dating the 1700 cascadia earthquake, *Nature*, *389*(6654), 922–923, 1997.